

ISOTOPE SHIFT AND NEW FINE STRUCTURE IN  
NEUTRAL ATOMIC OXYGEN

---

by

John R. Holmes, Project Director

and

Lee W. Parker, Research Associate

---

Technical Report No. 4

on work done under contract with

the Office of Naval Research

Contract No. N6onr-238, Task Order III

Project Designation No. NR-019-110

June 15, 1953

---

Department of Physics

The University of Southern California

Los Angeles, California

# TABLE OF CONTENTS

CHAPTER	PAGE
ABSTRACT . . . . .	1
I. INTRODUCTION . . . . .	3
II. EXPERIMENTAL APPARATUS AND PROCEDURE . . . . .	6
III. RESULTS . . . . .	20
IV. DISCUSSION . . . . .	25
Theoretical outline . . . . .	26
Nuclear mass effect . . . . .	26
Normal mass effect . . . . .	27
Specific effect perturbation . . . . .	29
Use of the sum rule . . . . .	32
One-electron matrix elements . . . . .	36
Specific isotope shift parameters for oxygen	38
Comparison of theoretical predictions	
with experimental results in oxygen . . . . .	41
Transition probability and f-value . . . . .	46
Comparison of oxygen with nitrogen . . . . .	48
V. NEW FINE STRUCTURE . . . . .	50
Experimental procedure . . . . .	51
$\lambda 8446$ . . . . .	51
$\lambda 2884$ . . . . .	52
$\lambda 4368$ . . . . .	52
Results . . . . .	56
Discussion . . . . .	57
REFERENCES . . . . .	61

# LIST OF TABLES

TABLE		PAGE
I.	Isotope Shifts in Oxygen of $O^{18}$ Relative to $O^{16}$ in Wave Numbers . . . . .	21
II.	Classification of Eigenfunctions of the Configuration $2p^3ns$ for Use of Energy Sum Rule . . . . .	40
III.	Comparison of Observed and Normal Relative Shifts in Pairs of $3p$ Levels . . . . .	42
IV.	Predicted Versus Observed Specific Shifts . . .	44
V.	New Fine Structure in Neutral Atomic Oxygen . .	54

# LIST OF FIGURES

FIGURE		PAGE
1.	Vacuum System and Discharge Tube Connections . .	7
2.	Optical System . . . . .	9
3.	Mirror Evaporation Scheme and Detail of Crucible	11
4.	Interferometric Patterns of $\lambda 8820$ Showing Isotope Structure . . . . .	12
5.	Densitometer Traces of $\lambda 8820$ . . . . .	13
6.	Isotope Structure in $\lambda 8446$ with 5 mm Spacer . . .	15
7.	Isotope Structure in $\lambda 8446$ with 6 mm Spacer . . .	16
8.	Isotope Structure in $\lambda 4368$ . . . . .	18
9.	O I Systems Showing Lines Examined for Isotope Shift . . . . .	24
10.	Fabry-Perot Fringes Showing All Three Components of $\lambda 8446$ . . . . .	53
11.	Energy Level Diagram for O I Showing Fine Structure Transitions Studied and the Deduced Structures of $3p \ ^3P_{210}$ and $4p \ ^3P_{210}$ . .	60



## ABSTRACT

An  $O^{18}$ -enriched oxygen gas sample has been used for examination of isotope structure in 20 atomic lines between 2000 and 10,000 Å. Strong sharp lines were obtained in a liquid nitrogen-cooled electrodeless quartz discharge tube containing up to 0.5 mm of oxygen in 5 mm of helium. Excited by a 10 mc oscillator, the discharge was photographed through an external Fabry-Perot interferometer in series with a large prism spectrograph. The shifts found ranged from zero to as high as  $0.5 \text{ cm}^{-1}$  for  $\lambda 4233 (4p \ ^3P - 3d' \ ^3P)$  and  $\lambda 2884 (3p \ ^3P - 3d' \ ^3P)$ .

Enough data was available to allow a study of the internal consistency of the measured shifts as a test of the mass effect theory. Relative shifts between pairs of  $3p$  levels were studied for conformity with the prediction that they should be given by the normal mass effect alone. Moreover, the data for two lines gave empirical values for specific effect integrals which were then used to predict shifts in other lines having known shifts. Both tests were favorable. The formal relationship of one of these integrals to radiation theory suggested the calculation of a transition probability and an  $f$  value for the  $\lambda 1306$  resonance triplet, resulting in reasonable values. It was concluded that the mass effect theory is generally applicable to oxygen, and that the abnormally large shifts found for  $\lambda 4233$  and  $\lambda 2884$  are the result of interactions affecting the common upper level. A comparison was made with earlier nitrogen data.

During the isotope shift survey, untabulated fine structure was resolved in the triplet multiplets

$\lambda 8446$  ( $3s\ ^3S_1 - 3p\ ^3P_{210}$ ),  $\lambda 2884$  ( $3p\ ^3P_{21} - 3d\ ^3P_2$ ), and  $\lambda 4368$  ( $3s\ ^3S_1 - 4p\ ^3P_{210}$ ).

Listed as a doublet,  $\lambda 8446$  has three components whose relative intensities allowed establishment of the  $3p\ ^3P$  anomalous splitting as follows:  $J = 1$  lies  $0.559\text{ cm}^{-1}$  below  $J = 2$ , and  $J = 0$  lies  $0.158\text{ cm}^{-1}$  above  $J = 2$ , in agreement with Edlén.  $\lambda 2884$ , heretofore found single, has two components separated by  $0.558\text{ cm}^{-1}$ , confirming the  $\lambda 8446$  data.

Two components of  $\lambda 4368$ , previously considered single, were resolved and found to have a separation of  $0.300\text{ cm}^{-1}$ , the weaker component having the shorter wavelength. From the relative intensities it was deduced that  $J = 0$  lies above the degenerate  $J = 2, 1$  level of the  $4p\ ^3P$  state.

## CHAPTER I

### INTRODUCTION

Interest in the hyperfine structure of atomic spectra has been recently stimulated by the availability of isotopes in pure form.<sup>1</sup> The two main nuclear effects involved, namely, the magnetic interaction due to a nuclear magnetic moment, and the isotope shift, are being studied for additional clues to the structure of nuclei. The hyperfine structure of any line generally consists of one component for each isotope of zero spin, usually of even mass, and a set of magnetic hyperfine components for each isotope with spin, usually of odd mass. The isotope shifts are then the relative differences in wave number among the single components of the even isotopes and the centroids of the odd isotopes, the determination of the centroids requiring a magnetic hyperfine term analysis.

It was found that the displacements of the deuterium satellites of the principal hydrogen lines<sup>2</sup> could be explained merely by using the reduced mass of the electron. A more general theory was first formulated for two- and three-electron atoms,<sup>3</sup> and was later extended to  $n$ -electron atoms.<sup>4</sup> With neglect of non-electrostatic interactions such as spin-orbit coupling the energy level correction consists of the sum of two parts, both of which are inversely proportional to the nuclear mass: The first is the change introduced by multiplying the levels for infinite nuclear mass by  $\mu/m$ , as was done for hydrogen and hydrogen-like ions; this part is called the normal mass effect. The second part arises in the many-body problem as a result of the transformation from laboratory coordinates to coordinates of the center

of mass and relative coordinates of the electrons with respect to the nucleus. The Hamiltonian becomes essentially hydrogen-like except for extra terms which couple pairs of electron momenta and which are treated as a perturbation. This is the specific mass effect and is very difficult to evaluate, requiring a precise knowledge of the wave functions of the particular levels involved. Contributions of the specific effect have been calculated for transitions in the spectra of  $\text{Li}^3$ ,  $\text{Ne}^4$ ,  $\text{Mg}^5$ ,  $\text{B}^6$ , and  $\text{He}^7$ . There is fair agreement with experiment for roughly half of all shifts predicted, and poor agreement for the rest. Where discrepancies occur, there is doubt as to the precision of the wave functions used, as well as to the justification of the neglect of spin-orbit coupling.

The large displacements and non-linear spacings of isotopic components found in heavy element spectra cannot be accounted for by the mass effect, which should be vanishingly small there. A fairly consistent explanation is based on the hypothesis of the existence of a non-Coulomb field experienced by an electron which penetrates the extended volume of the nucleus. This nuclear field theory has been applied with some success to the spectra of heavy elements.<sup>8</sup>

For elements of intermediate atomic number a superposition of the mass and field effects has been assumed to be valid. Unfortunately, as a result of the mathematical difficulties very few calculations of the mass effect for such elements have been made to test the correctness of this assumption. From a consideration of the shifts found in the Zn spectrum, however, Crawford

et al. conclude that the contribution from the specific mass effect may be relatively appreciable despite the large nuclear mass.<sup>9</sup>

The existing discrepancies with theory are sufficient to warrant the accumulation of more experimental isotope shift data, for the light as well as for the heavy elements. This report consists mainly of an exposition of isotope shift measurements on oxygen and a semi-quantitative theoretical analysis.<sup>10</sup> In addition, there is reported some new fine structure discovered during the isotope shift survey.<sup>11</sup> An analysis of this structure is made to infer the splittings of the energy levels involved.

## CHAPTER II

### EXPERIMENTAL APPARATUS AND PROCEDURE

The measurements were made with oxygen gas enriched with about 29 per cent  $O^{18}$ , kindly furnished by A. O. Nier. By the use of an electrodeless discharge in a quartz tube containing an oxygen-helium mixture sharp interferometric patterns could be photographed generally with less than an hour of exposure, even for the weaker lines.

Figure 1 shows the vacuum system used and the electrical connections to the discharge tube, the lower half of which was made narrow for effective cooling. A 10 mc power oscillator excited the discharge. Liquid nitrogen cooling, in addition to minimizing the Doppler broadening, enhanced the atomic spectrum relative to the band background since even with cold traps on the system sufficient stopcock grease vapor could enter the discharge to produce numerous impurity bands, which were suppressed if the discharge tube were kept sufficiently cool.

Owing to the small but not negligible clean-up of oxygen which occurred with time, a discharge was run with the pure oxygen isotope mixture, with fresh oxygen being added a little at a time until the walls of the tube became thoroughly impregnated with the mixture and the pressure remained constant. A Pirani gauge was used to measure the oxygen pressure since mercury reacted with the oxygen strongly enough to cause large fluctuations in the concentration. It was found that relatively high oxygen concentrations (roughly 0.5 mm of  $O_2$  in 5 mm of He) were necessary for optimum brightness of the atomic spectrum. (If the

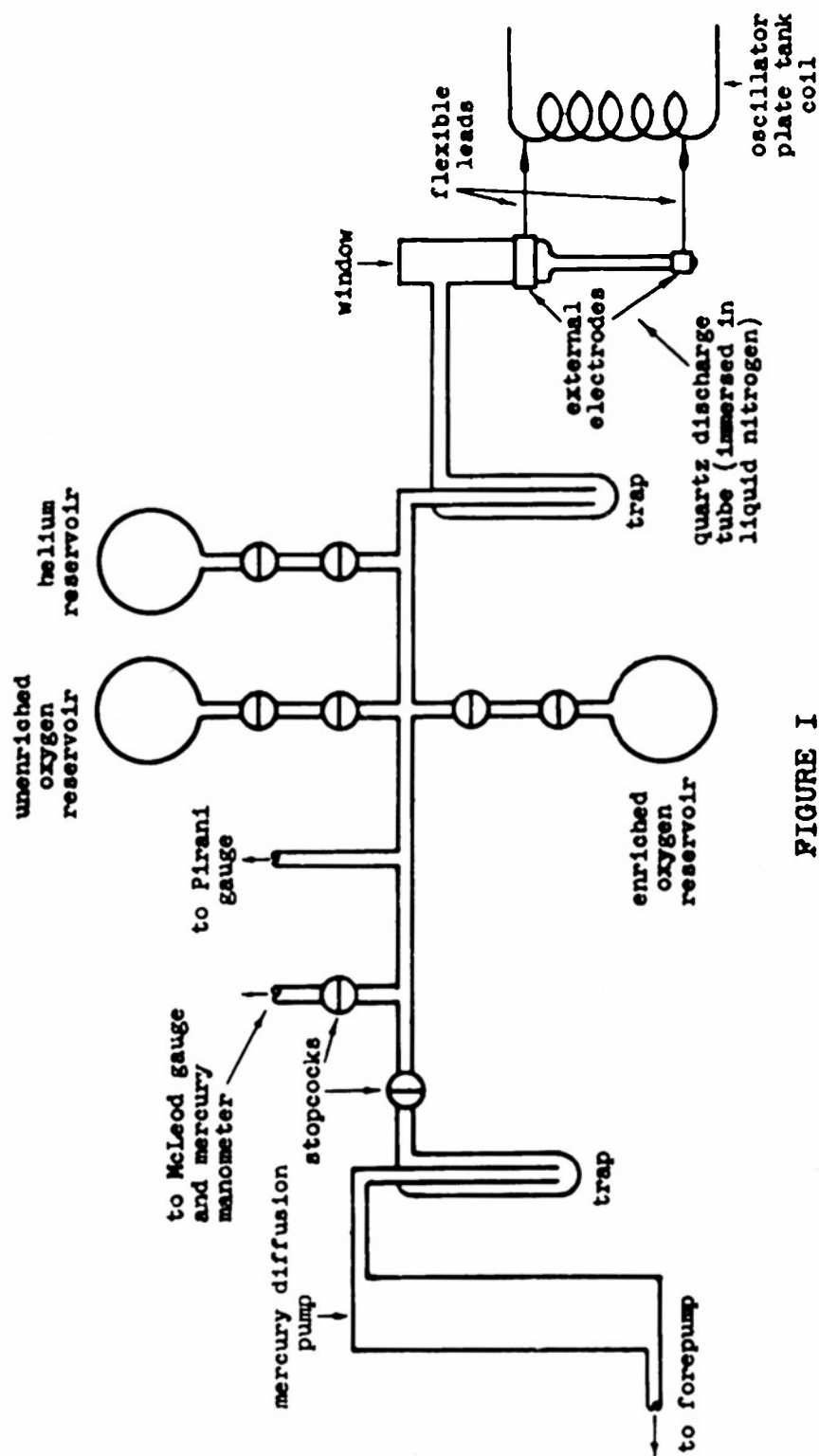


FIGURE I

VACUUM SYSTEM AND DISCHARGE TUBE CONNECTIONS

concentration were allowed to decrease to zero by means of the clean-up process, the bands would become relatively stronger than the lines and would vanish no more rapidly than the strongest lines.)

To maintain a stable bright plasma, a minimum power input, depending on the oxygen concentration, was required. That is, for a given mixture there was a minimum oscillator plate voltage at which the bright plasma appeared. For strong lines, a small oxygen concentration (less than 0.1 mm) could be used, with a correspondingly low power input. When the best oxygen-helium mixture was achieved, the discharge had an orange color, Helium 5876 and Oxygen 6158 appearing equally bright to the eye. The minimum plate voltage required to maintain a stable bright plasma was always used, to keep the power dissipation low without an appreciable sacrifice in brilliance.

Lines in the wavelength range 2000A to 10,000A were studied by means of a Fabry-Perot interferometer the auxiliary crossed dispersion for which was provided by a large Hilger E1 quartz-glass prism spectrograph. The interferometer was mounted external to the spectrograph in a parallel beam arrangement. An auxiliary slit between the source and the interferometer was found necessary for the elimination of spurious fringes produced by the interferometer plates.<sup>12</sup> The optical system is shown in Figure 2.

A pair of silvered interferometer plates was used for the visible and infrared, and aluminized plates for the ultraviolet. The silver films were re-evaporated when necessary to obtain optimum performance for lines of different intensity.



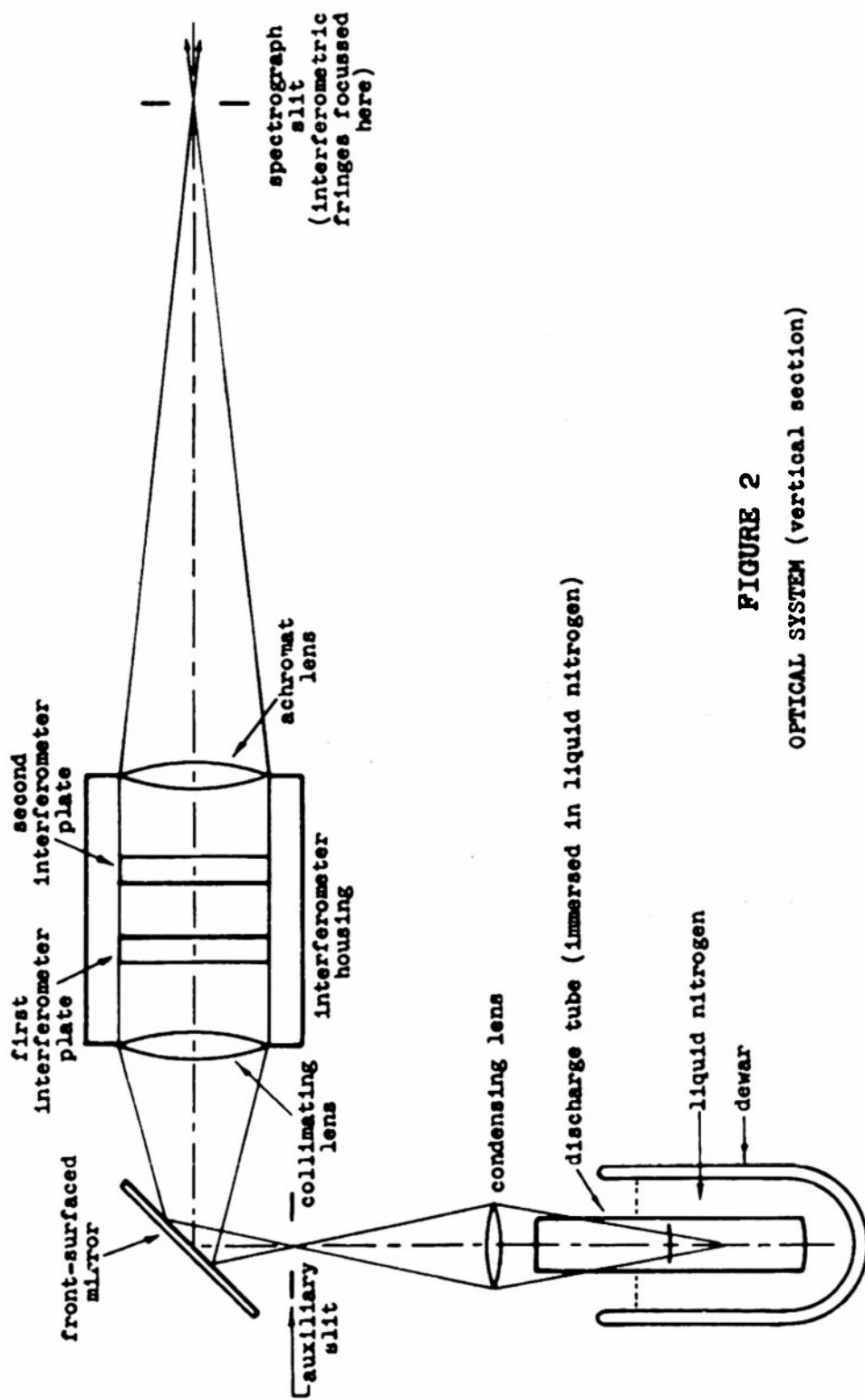


FIGURE 2

OPTICAL SYSTEM (vertical section)

A single set of aluminum films, however, sufficed throughout the work. Figure 3 shows the evaporation scheme and crucible used in the preparation of the silver films, for which the data of Kuhn and Wilson<sup>13</sup> served as a valuable guide.

For the violet and ultraviolet regions, Eastman O plates were used, and for the near infrared (in which region many important oxygen lines occurred) hypersensitized Eastman N plates were found excellent.

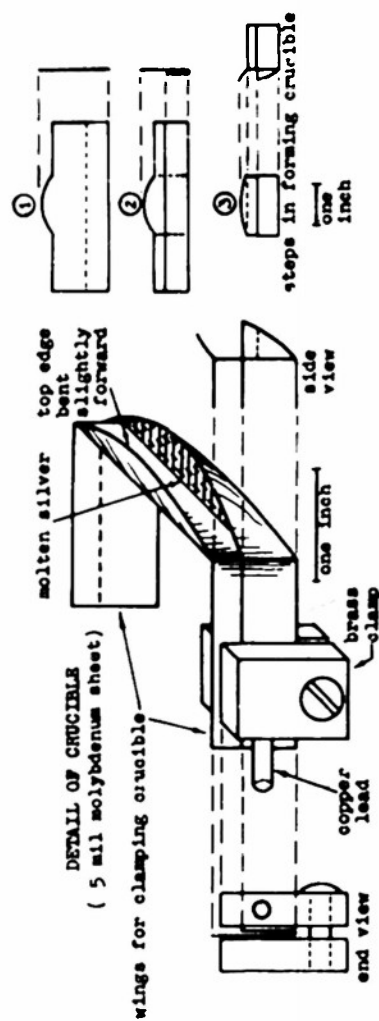
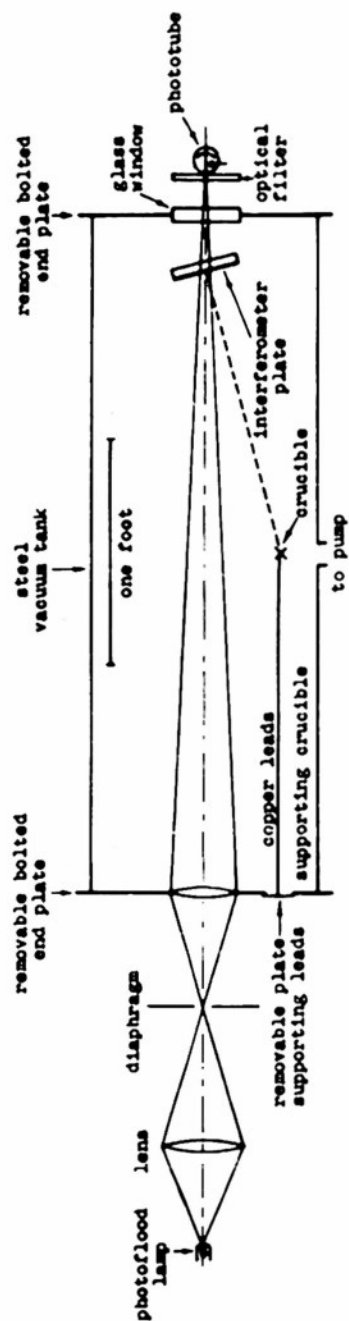
Where lines could be photographed with a wide slit, a Zeiss microphotometer connected to a Speedomax Leeds and Northrup recorder reproduced the interferometric pattern contours. In cases where a narrow slit was required, the positions of the peaks were determined with a traveling comparator microscope. The isotope shift in a given line was found by measuring the relative positions of the  $O^{18}$  and  $O^{16}$  peaks in the pattern and using MacNair's method for calculating the shifts in terms of fractions of an order.<sup>14</sup> This method was found to be faster and no less accurate than second-degree interpolation.

Since the techniques varied among the various lines and line groups, they are here individually discussed.

$\lambda 3820$ : This strong single line was easiest to photograph, resulting in a very accurate measurement. Figure 4 shows the  $O^{18}$  satellite with two different spacers and Figure 5 exhibits corresponding densitometer traces.

$\lambda 8446$ :<sup>15</sup> Use of a small spacer reduced the confusion caused by the triplet fine structure. 5 and 6 mm spacers allowed all three fine structure components and their  $O^{18}$  satellites

MIRROR EVAPORATION SCHEME



MIRROR EVAPORATION SCHEME AND DETAIL OF CRUCIBLE

FIGURE 3

# INTERFEROMETRIC PATTERNS OF $\lambda 8820_{(\text{SINGLET})}$ SHOWING ISOTOPE STRUCTURE

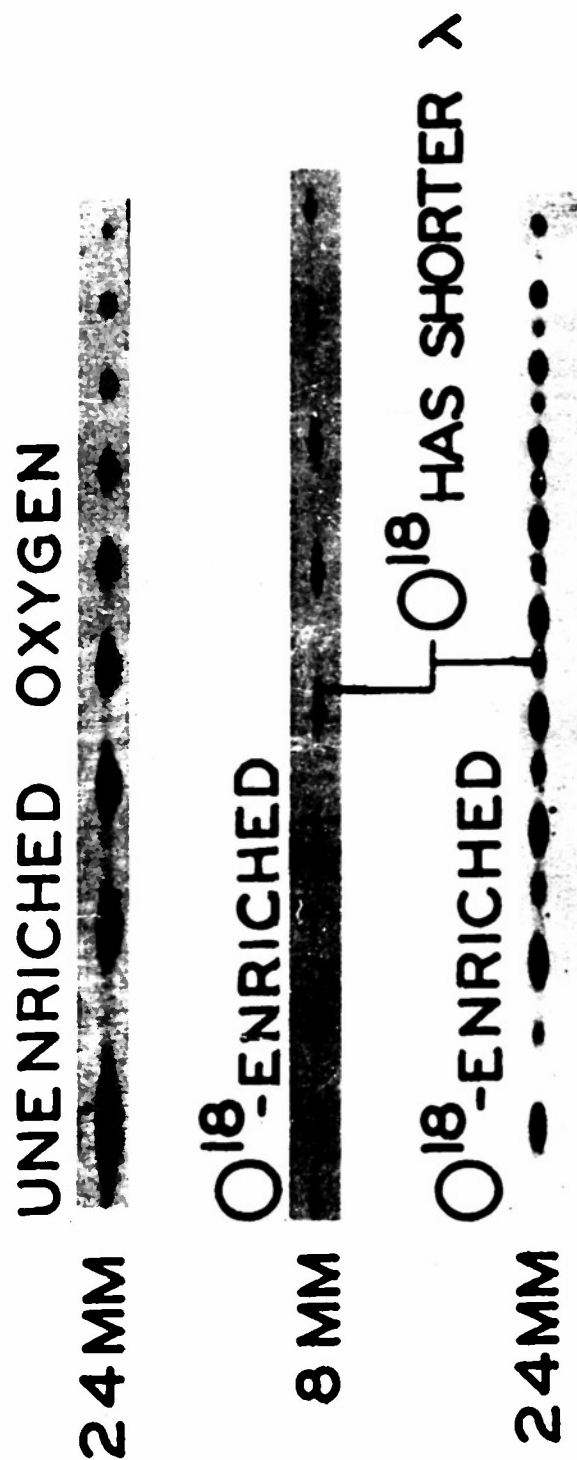


FIGURE 4

STRUCTURE OF OI 8820.45  
FOR O<sup>18</sup>-ENRICHED MIXTURE

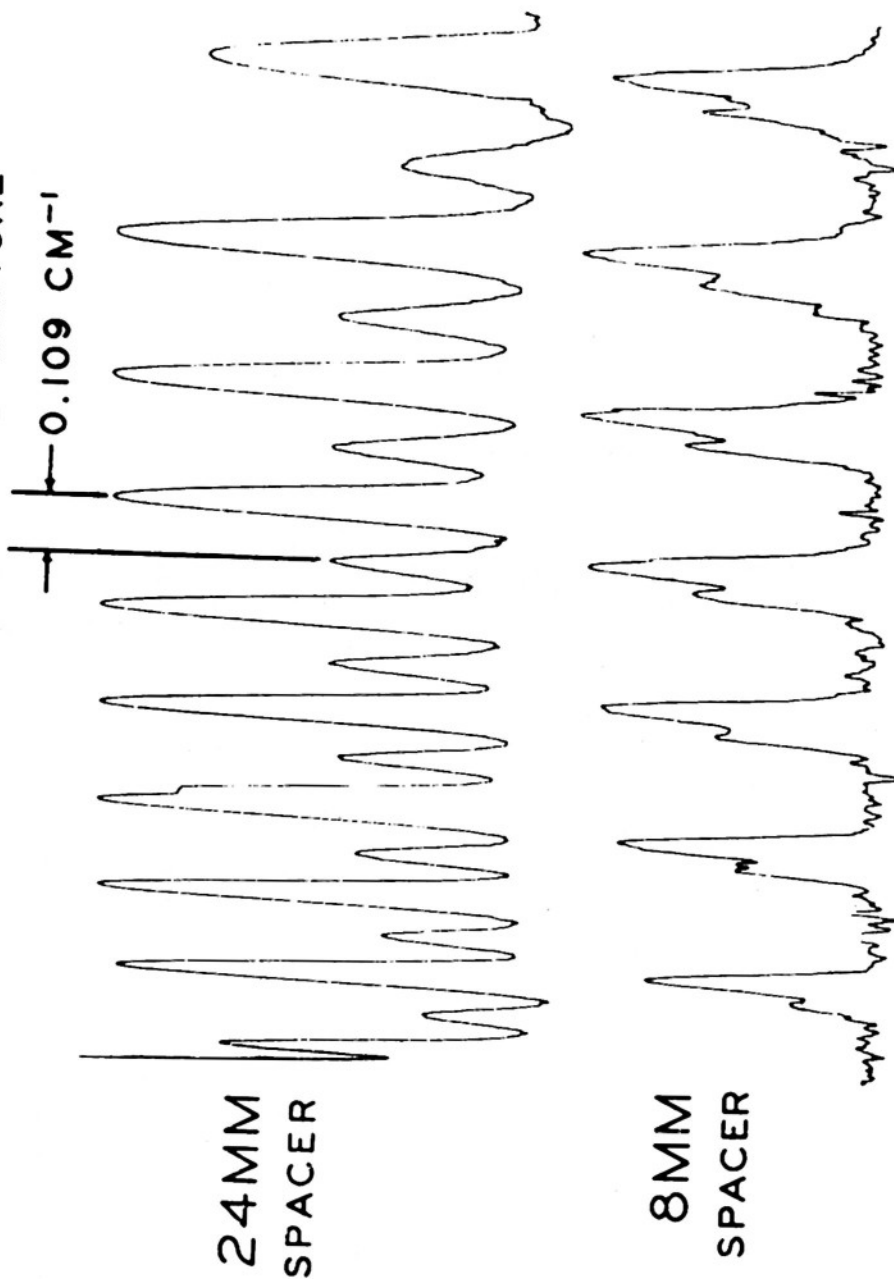


FIGURE 5  
DENSITOMETER TRACES OF  $\lambda 8820$

to be accounted for. Figures 6 and 7 show the isotope structure of this very strong line.

$\lambda 8222$ : Among the members of the multiplet, which were just resolved by the spectrograph, this wavelength and  $\lambda 8233$  appeared strongly enough to measure. Use of a wide slit was possible.

$\lambda 7995$ : This line was quite faint and very close to a strong line of argon, which was present as a contaminant in the enriched sample. It required a run of several hours with a narrow slit, and showed an asymmetry toward long wavelengths with a 46 mm spacer. Only one component of the multiplet listed<sup>16</sup> appeared.

$\lambda 7772$ : Its lower level being metastable, this strong triplet, which could just be resolved with a narrow slit, showed marked self-reversal with a thick source. The strength of the line allowed the use of a narrow tube which was observed side-on while completely immersed in liquid nitrogen.

$\lambda 7476$ : Only one component of the listed multiplet appeared.<sup>16</sup> The largest spacer used, 46 mm, failed to show up any asymmetry.

$\lambda 7157$ : Several hours of exposure were needed for this very faint single line. The  $O^{18}$  satellite appeared clearly with an 8 mm spacer, but hazily with larger spacers.

$\lambda 7002$ : With an 8 mm spacer, all three components were exactly superimposed. Since any asymmetry would have been noticeable, an upper limit could be assigned to the isotope shift.

# ISOTOPE STRUCTURE IN $\lambda$ 8446 (TRIPLET) 5 MM SPACER

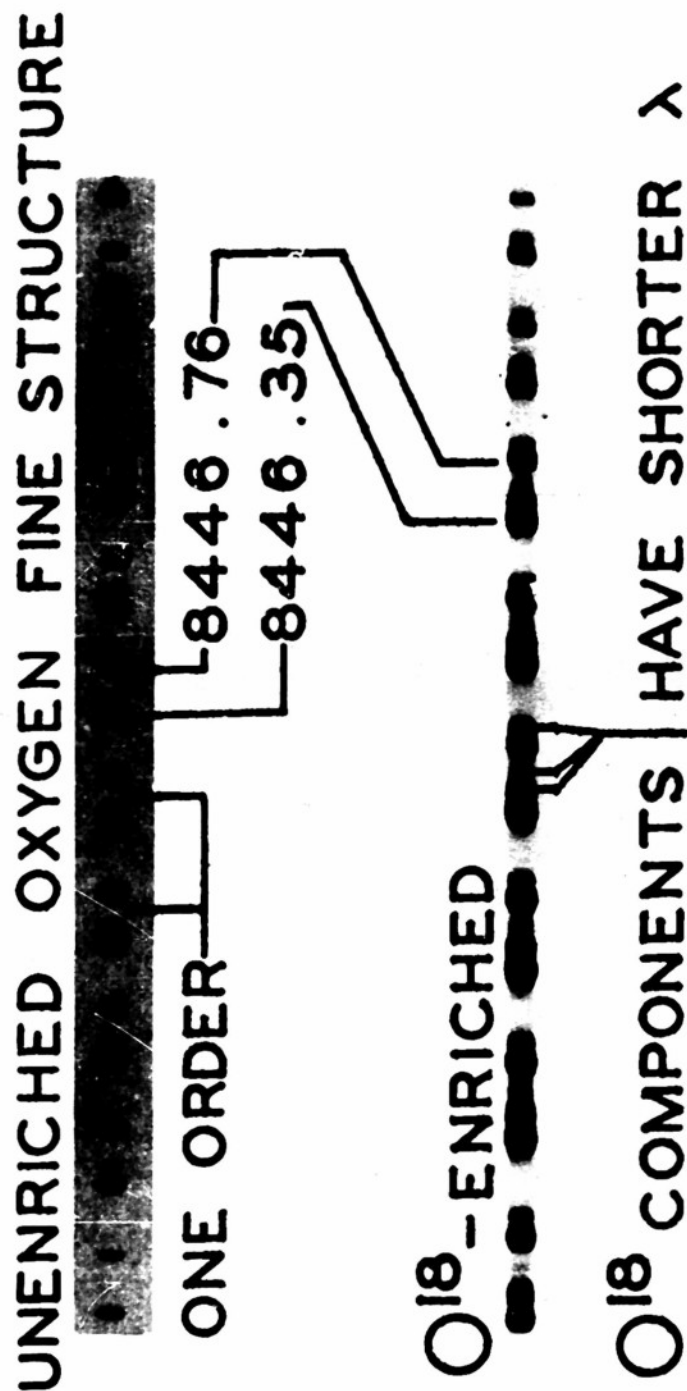


FIGURE 6

# ISOTOPE STRUCTURE IN $\lambda 8446$ (TRIPLET) 6MM SPACER

UNENRICHED OXYGEN FINE STRUCTURE  
ALONE

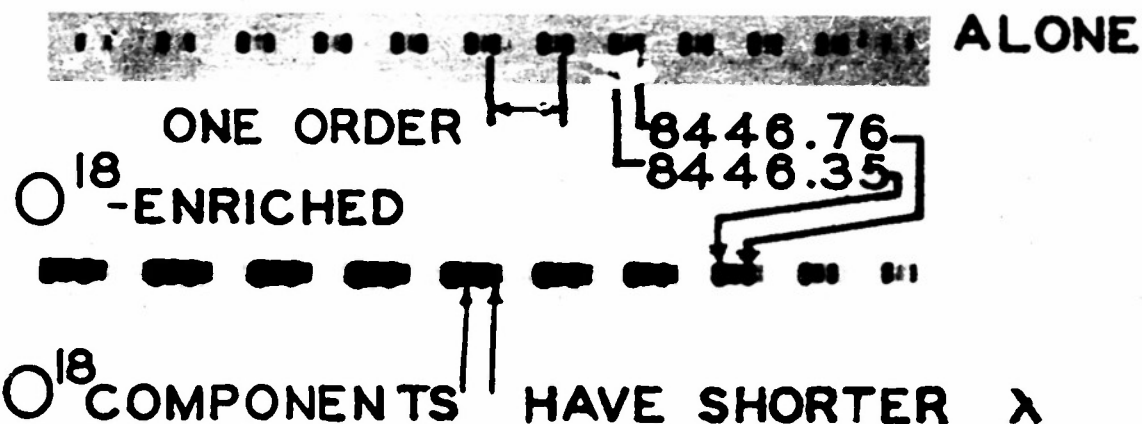


FIGURE 7



# ISOTOPE STRUCTURE IN $\lambda 8446$ (TRIPLET) 6MM SPACER

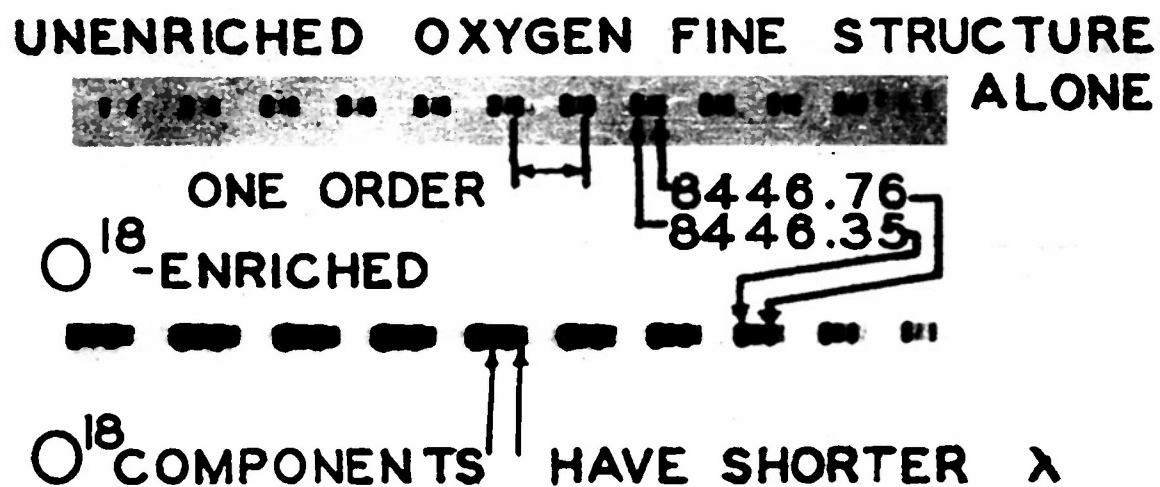


FIGURE 7

$\lambda\lambda 6456, 6158, 5437, 5331, \text{ and } 4969$ : At least one component of each of these triplets was just resolved from the others with a narrow slit.  $\lambda 6456$  and  $\lambda 6158$  were sharp enough to allow use of a 46 mm spacer.

$\lambda 4368$ : Listed as a single line,<sup>16</sup> this strong multiplet was found to have two fine structure components whereas three are expected from the transition. Fortunately the fine structure splitting was about double the isotope splitting, so that the  $O^{18}$  satellite of the strong component could be displaced about half an order with an appropriate spacer, while the weak fine structure component was separated by exactly one order. See Figure 8.

$\lambda 4233$ : This faint line had some band background which was slightly less intense than the  $O^{18}$  satellite. With a narrow slit an hour of exposure was required.

$\lambda 3955$ : The only two components observed were so staggered in wavelength that an 8 mm spacer could be used to assign an upper limit to the shift.

$\lambda 3947$ : Although three components appeared, a comparison of exposures with enriched and unenriched oxygen showed an asymmetry when an 8 mm spacer was used.

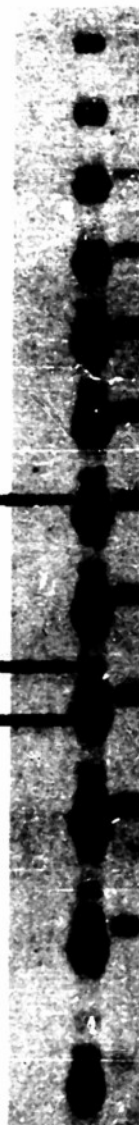
$\lambda 3823$ : The strongest component of a resolved multiplet, this line showed an  $O^{18}$  satellite clearly with an 8 mm spacer, but hazily with larger spacers. A narrow slit had to be used.

$\lambda 3692$ : The same behavior was shown by this line.

$\lambda 2884$ : Due to the considerable band background in this region,

# ISOTOPE STRUCTURE

IN  $\lambda$  4368  
(INCOMPLETELY RESOLVED TRIPLET)  
8 MM  $O^{16}$   $O^{18}$



16 MM  $O^{16}$   $O^{18}$



$O^{18}$  COMPONENT HAS SHORTER  $\lambda$

FIGURE 8

the positions of the  $O^{18}$  satellites of the two newly resolved triplet components<sup>16</sup> were inferred from comparison of intensity pattern contours of identical exposures with enriched and unenriched oxygen. The value obtained was consistent with that predictable from consideration of the closed quadrilateral formed by  $\lambda\lambda 2884, 8446, 4368,$  and  $4233$ .

## CHAPTER III

### RESULTS

Table I lists the lines studied, with transitions and isotope shifts. An unprimed symbol for the optical electron refers to a level in the  $^4S$  system, which is built on the  $^4S$  term of the ion. Primed and double-primed symbols refer to the  $^2D$  and  $^2P$  systems, respectively. The errors given for the various measured shifts are estimates of the maximum range of error. Although it is conventional to give the probable rather than the maximum error, it was uncertain whether all systematic errors could be accounted for. As an example, a band line unsymmetrically superimposed on the  $O^{18}$  satellite could, even if lower in intensity, introduce a systematic spurious shift in all orders of a pattern. The probable error in such a case could be very small for that set of data, and therefore be misleading. It was decided to list estimated maximum errors for all lines instead of risking confusion by listing probable errors for some and maximum errors for others. In all cases, the probable error was of the order of several times smaller than the maximum error, which was estimated high. Each observed shift given to three decimal places is the average of around 12 determinations, taken from one or two plates. For these lines the spacer was always chosen so that the  $O^{18}$  satellite, for the final plates, lay approximately midway between orders. The symmetry thus imposed prevented spurious shifting of the peaks relative to each other due to overlapping of the wings. Shifts given to less than three decimal places involved some difficulty in assignment of exact values because of

TABLE I

ISOTOPE SHIFTS IN OXYGEN OF  $O^{18}$  RELATIVE TO  $O^{16}$  IN WAVE NUMBERS<sup>a</sup>

No.	Wavelength	Transition	Observed Shift	Normal	Residual
1	7771.96	$3s\ ^5S_2 - 3p\ ^5P_3$	$0.065 \pm 0.003$	0.049	$0.013 \rightarrow 0.019$
2	3947.30	$3s\ ^5S_2 - 4p\ ^5P_3$	$\lesssim 0.1$	0.10	$\lesssim 0$
3	8446.76	$3s\ ^3S_1 - 3p\ ^3P_1$	$0.14 \pm 0.01$	0.05	$0.08 \rightarrow 0.10$
4	4368.30	$3s\ ^3S_1 - 4p\ ^3P_{21}$	$0.141 \pm 0.003$	0.087	$0.051 \rightarrow 0.057$
5	3692.44	$3s\ ^3S_1 - 5p\ ^3P_{210}$	$0.15 \pm 0.02$	0.10	$0.03 \rightarrow 0.07$
6	6456.01	$3p\ ^5P_3 - 5s\ ^5S_2$	$< 0.02^b$	0.06	$-0.08 \rightarrow -0.04$
7	6158.19	$3p\ ^5P_3 - 4d\ ^5D_{432}$	$< 0.03^b$	0.06	$-0.09 \rightarrow -0.03$
8	5436.83	$3p\ ^5P_3 - 6s\ ^5S_2$	$< 0.02^b$	0.07	$-0.09 \rightarrow -0.05$
9	5330.66	$3p\ ^5P_3 - 5d\ ^5D_{432}$	$< 0.03^b$	0.07	$-0.10 \rightarrow -0.04$
10	4968.76	$3p\ ^5P_3 - 6d\ ^5D_{432}$	$< 0.04^b$	0.08	$-0.12 \rightarrow -0.04$

<sup>a</sup>All values are positive unless otherwise indicated.<sup>b</sup>In magnitude.

TABLE I (continued)

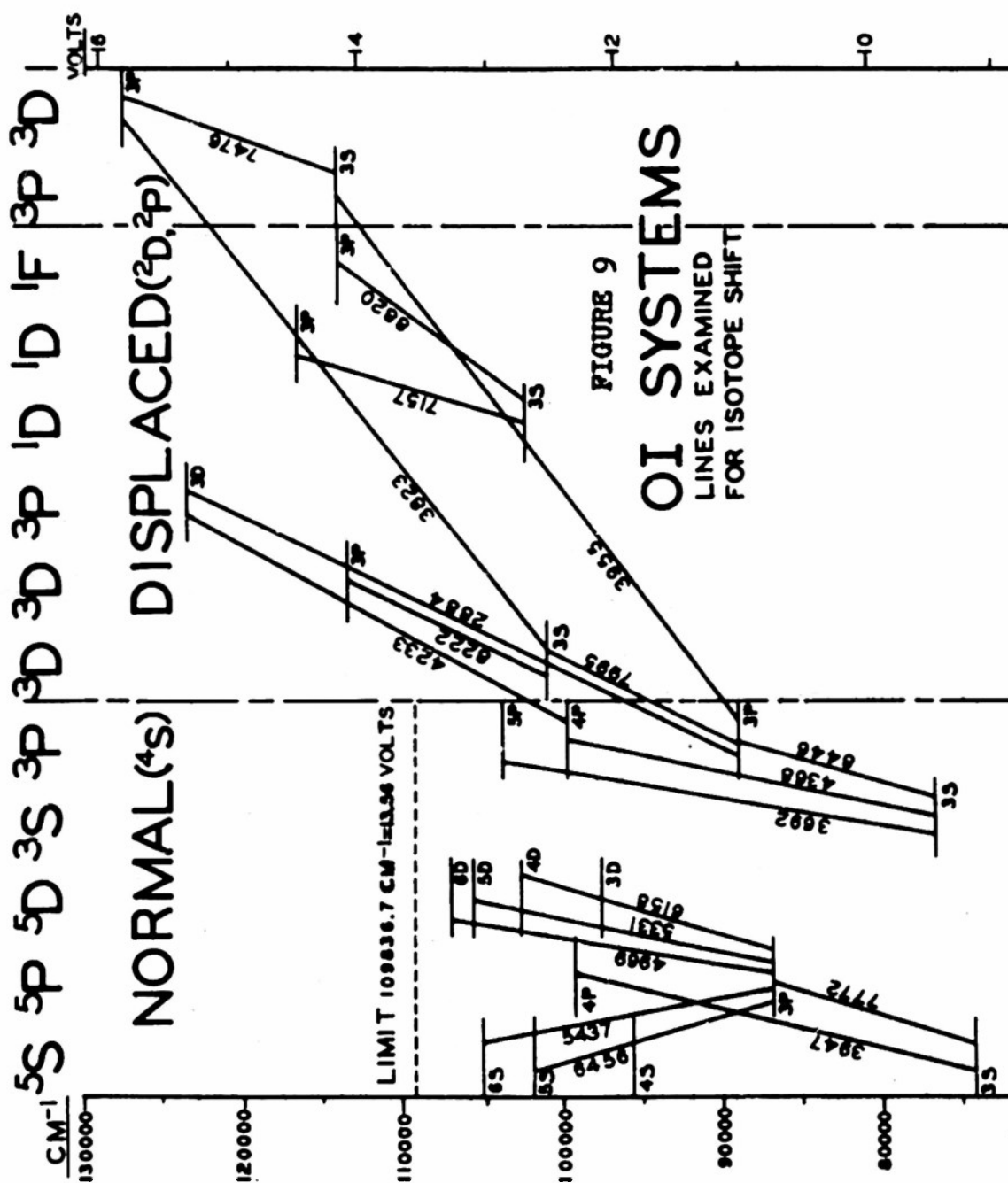
No.	Wavelength	Transition	Observed Shift	Normal	Residual
11	3954.69	$3p\ ^3P_2 - 3s''\ ^3P_2$	$<0.1^b$	0.10	$-0.2 \rightarrow 0$
12	4233.32	$4p\ ^3P_{21} - 3d'\ ^3P_2$	$0.47 \pm 0.02$	0.09	$0.36 \rightarrow 0.40$
13	8221.84	$3s'\ ^3D_3 - 3p'\ ^3D_{32}$	$0.083 \pm 0.003$	0.046	$0.074 \rightarrow 0.040$
13a	8232.99	$1\ ^3D_3$	$0.083 \pm 0.004$	0.046	$0.073 \rightarrow 0.041$
14	3823.47	$3s'\ ^3D_3 - 3p''\ ^3D_3$	$0.14 \pm 0.01$	0.10	$0.03 \rightarrow 0.05$
15	8820.45	$3s'\ ^1D_2 - 3p'\ ^1P_3$	$0.109 \pm 0.002$	0.043	$0.064 \rightarrow 0.068$
16	7156.80	$3s'\ ^1D_2 - 3p'\ ^1D_2$	$0.11 \pm 0.01$	0.05	$0.05 \rightarrow 0.07$
17	7476.45	$3s''\ ^3P_2 - 3p''\ ^3D_3$	$<0.01^b$	0.05	$-0.06 \rightarrow -0.04$
18	2883.78	$3p\ ^3P_{21} - 3d'\ ^3P_2$	$0.50 \pm 0.05$	0.13	$0.32 \rightarrow 0.42$
19	7995.12	$3p\ ^3P_2 - 3s'\ ^3D_3$	$-0.01 \rightarrow -0.02$	0.05	$-0.07 \rightarrow -0.06$
20	7002.22	$3p\ ^3P_{20} - 4d\ ^3D_{321}$	$<0.1^b$	0.05	$-0.05 \rightarrow +0.05$

excessive band background, haziness, or interfering fine structure. The signs applied follow the convention that a shift to higher frequencies in going from  $O^{16}$  to  $O^{18}$  is called positive. The normal mass effect, always positive was calculated in the usual way with the formula:

$$\Delta\nu = \frac{\Delta\mu}{m} \nu \quad (1)$$

where  $\Delta\mu$  is the reduced mass change from that of  $O^{16}$  to that of  $O^{18}$ ,  $m$  is the electron mass, and  $\nu$  is the wave number of the transition in  $O^{16}$ . Given in the last column of Table I are the differences between the observed and normal shifts. These should correspond to the specific mass effect, since no other theoretical significance has been suggested for the residual shifts found in light elements. An energy level diagram with the transitions giving rise to the investigated lines is shown in Figure 9. Two quadrilateral figures, it may be noted, are formed by the two respective sets of wavelengths:  $\lambda 4233$ ,  $\lambda 4368$ ,  $\lambda 8446$ ,  $\lambda 2884$ , and  $\lambda 3823$ ,  $\lambda 7995$ ,  $\lambda 3955$ ,  $\lambda 7476$ . These closed polygons afford a check on the internal consistency of the measured shifts. Although the shifts in lines forming the first quadrilateral are energetically consistent, those in the second quadrilateral are not. In connection with the latter inconsistency, the classification of the transition  $\lambda 7476$  is questioned in the following theoretical discussion, in which an outline of the mass effect theory is given and an attempt, based on the observed shifts, is made to justify the applicability of the theory to oxygen.





## CHAPTER IV

### DISCUSSION

For the purpose of testing strictly the validity of the mass effect theory of Hughes and Eckart,<sup>3</sup> it is necessary that certain integrals be evaluated in the calculation of the specific mass effect. As in the Slater-type perturbation calculation of Russell-Saunders term energies,<sup>17</sup> the problem is two-fold: The first part consists of the establishment of the desired perturbation energies in terms of linear combinations of unevaluated integrals, which are treated as algebraic parameters. The second part of the problem is that of obtaining the numerical values of the integrals. This requires a knowledge of the precise central-field wave functions for the particular states involved. The unavailability of the necessary wave functions for oxygen prevented the second part of the calculation from being executed. However, much could be done with the algebraic relationships of the first part. A sufficiently large number of measurements were made to allow the empirical evaluation of some of the parameters. The parameters thus evaluated were used to predict other shifts which had been experimentally observed. Such a procedure afforded a good internal consistency test of the theory.

In the following derivation of the mass effect corrections, some familiarity with the elementary perturbation theory of quantum mechanics is assumed. After an outline of the general theory has been presented, the specific isotope shift parameters for oxygen are deduced and an internal consistency test of the theory

is made. Since some isotope shift data for nitrogen is available, a comparison between corresponding parameters for oxygen and nitrogen is possible. Of additional interest is the relationship of the specific isotope shift integrals to radiation theory dipole moment integrals. By making use of this relationship, an approximate calculation of the transition probability and oscillator strength for the  $\lambda 1306$  resonance triplet of oxygen can be effected and should yield reasonable values if the mass effect theory is applicable.

### I. THEORETICAL OUTLINE

Nuclear mass effect. The theoretical treatment of isotope shift requires that the mass of the nucleus be incorporated into the Hamiltonian of the system, and thus into the expression for the energy of a given state. Hence, the kinetic energy expression will have a term for the motion of the nucleus in addition to the terms for the electrons. In the laboratory system the classical kinetic energy is given by:

$$T = (m/2) \sum_{i=1}^t \dot{\vec{s}}_i^2 + (M/2) \dot{\vec{S}}^2$$

where  $m$  and  $\vec{s}_i$  are the mass and coordinate vector, respectively, of the  $i^{\text{th}}$  electron,  $M$  and  $\vec{S}$  are the mass and coordinate vector, respectively, of the nucleus, and  $t$  is the number of electrons. The most natural coordinates for this problem, however, are the coordinates of the electrons relative to the nucleus and the coordinates of the center of mass. If the transformation to center of mass coordinates  $(\vec{R})$  given by

$$(M + tm)\vec{R} = M\vec{S} + m \sum_{i=1}^t \vec{s}_i$$

and to relative coordinates ( $r_1$ ) given by

$$\vec{r}_1 = \vec{s}_1 - \vec{s}, \quad 1 = 1, 2, \dots, t$$

is effected, and if  $\vec{p}_1$  and  $\vec{P}$  be the momenta conjugate to  $\vec{r}_1$  and  $\vec{R}$ , respectively, the following expression results for the classical Hamiltonian:

$$H = (1/2\mu) \sum_{i=1}^t p_i^2 + (1/M) \sum_{i>j} \vec{p}_i \cdot \vec{p}_j + P^2/2(M + tm) + V$$

where  $\mu$  is the reduced mass  $mM/(m + M)$ . In the absence of an external field, the potential  $V$  will not contain the center of mass coordinates. As a result, the corresponding Schrödinger equation

$$\left\{ -\frac{\hbar^2}{2\mu} \sum_{i=1}^t \nabla_i^2 - \frac{\hbar^2}{M} \sum_{i>j} \nabla_i \cdot \nabla_j - \frac{\hbar^2}{2(M+tm)} \nabla^2 + v \right\} \Psi = \omega \Psi,$$

is separable and  $\Psi$  may be written as the product  $\Xi(\vec{R})\psi(\vec{r}_1)$ . Correspondingly, the energy  $\omega = w + W$ , where  $w$  is associated with  $\Xi(\vec{R})$  and is determined by the equation for a free particle of mass  $(M + tm)$ :

$$-\frac{\hbar^2}{2(M+tm)} \nabla^2 \Xi = w \Xi$$

The remaining Schrödinger equation,

$$\left\{ -\frac{\hbar^2}{2\mu} \sum_i \nabla_i^2 - \frac{\hbar^2}{M} \sum_{i>j} \nabla_i \cdot \nabla_j + v \right\} \psi = w \psi, \quad (2)$$

describes the internal motion of the system and differs from the "normal" form by the presence of the terms in  $\nabla_i \cdot \nabla_j$ , which are responsible for that part of the isotope effect called the specific effect.

Normal mass effect. Neglecting the specific effect terms,

it will be demonstrated that the effect of nuclear motion can be expressed by the replacement of  $m$  by  $\mu$ , the reduced mass, in equation (2). The exact result of such a substitution is the replacement of  $W_0$ , the energy for a fixed nucleus, by the corrected energy  $W = W_0(1 + m/M)^{-1}$ . As will be shown, this follows from the fact that the potential energy  $V$ , assumed to be strictly Coulombic, is homogeneous in the coordinates and is of degree -1; i.e.,  $V(\xi x_1, \dots, \xi x_t) = \frac{1}{\xi} V(x_1, \dots, x_t)$ . If in the equation

$$\left\{ -\frac{\hbar^2}{2\mu} \sum_1 \nabla_1^2 + v \right\} \psi = W \psi \quad (3)$$

the transformation of variable  $x_1 = \xi x_1'$  is applied, then

$$\nabla_1^2 = \frac{1}{\xi^2} \nabla_1'^2 \quad \text{and}$$

$$\left\{ -\frac{\hbar^2}{2\mu \xi^2} \sum_1 \nabla_1'^2 + \frac{1}{\xi} v(x_1') \right\} \psi = W \psi$$

or

$$\left\{ -\frac{\hbar^2}{2\mu \xi} \sum_1 \nabla_1'^2 + v(x_1') \right\} \psi = \xi W \psi \quad (4)$$

Assuming the solution of (4) with  $\mu \xi = m$  and  $\xi W = W_0$  is known for the fixed nucleus, the energy in (3) is given by

$$W = \frac{1}{\xi} W_0 = \frac{\mu}{m} W_0$$

This is the normal mass effect.

Hence the normal correction for finite nuclear mass,  $\Delta W = W - W_0$ , is inversely proportional to the nuclear mass

because

$$\Delta W = W_0(1 + m/M)^{-1} - W_0 \approx W_0(1 - m/M) - W_0 = -\frac{m}{M} W_0$$

The normal correction is positive (energy levels are raised) since  $W_0$  is negative.

Specific effect perturbation. The specific effect terms,

$$\sigma = \frac{1}{M} \sum_{i>j} \vec{p}_i \cdot \vec{p}_j = -\frac{\hbar^2}{M} \sum_{i>j} \nabla_i \cdot \nabla_j$$

are now to be regarded as a perturbation, in exact analogy with the treatment of the inter-electron electrostatic repulsion terms  $\sum e^2/r_{ij}$  which appear in the potential function and lead to a splitting into Russell-Saunders terms when spin-orbit coupling is neglected.<sup>17</sup> In applying the perturbation technique, certain matrix elements of  $\sigma$  are needed and are constructed with approximate wave functions. The customary procedure is to assume that all electrons move in central Hartree fields without any mutual interactions. The wave functions and corresponding energy levels of any one of these electrons are characterized by the two quantum numbers  $n$  and  $\ell$ , the principal and orbital angular momentum quantum numbers, respectively. In the approximation that all such electrons move independently of one another, the Hamiltonian is separable; that is, the Hamiltonian is the sum of the individual Hamiltonians and the total energy is the sum of the individual energies. Correspondingly, the solution of the combined Schrödinger equation may be taken to be a product or a linear combination of products of one-electron wave functions.

The total energy in this approximation depends only on the set of  $n$ 's and  $\ell$ 's, which is called the configuration. However two more quantum numbers must be prescribed for each electron:

$m_l$  and  $m_s$ , referring to the orbital and spin angular momentum projections along the z-axis, respectively. These do not affect the energy, which is thus degenerate in this zero-order approximation. A zero-order wave function of a given configuration of  $t$  electrons consists of a product or a linear combination of products of  $t$  one-electron wave functions, each one-electron wave function being characterized by a set of four quantum numbers  $n, l, m_l, m_s$ . Suppose  $U$  is a zero-order wave function, characterized by the set of  $4t$  quantum numbers  $(n_1, l_1, m_{l1}, m_{s1}, \dots, n_t, l_t, m_{lt}, m_{st})$ , which belongs to the configuration  $(n_1, l_1, \dots, n_t, l_t)$ . The diagonal matrix element of the specific effect for that state is given by

$$(U|\sigma|U) = \frac{1}{M}(U|\sum_{1 \rightarrow j} \vec{p}_1 \cdot \vec{p}_j|U) \equiv -\frac{\hbar^2}{M} \sum_{1 \rightarrow j} \int U^* \nabla_1 \cdot \nabla_j U d\tau = \sigma_{UU}$$

It will now be shown that this matrix element vanishes for completely "independent" electrons.

One may write

$$\sigma_{UU} = +\frac{\hbar^2}{M} \sum_{1 \rightarrow j} \int \nabla_1 U^* \cdot \nabla_j U d\tau$$

by partial integration. Let  $U$  be given by the arbitrary product  $U = u_\alpha(1)u_\beta(2)\dots u_\rho(t)$ . The Greek letter subscript denotes a particular individual set of quantum numbers  $(n, l, m_l, m_s)$ , and the argument refers to the coordinates and spin of a particular electron. Thus,  $\sigma_{UU}$  is proportional to

$$\sum_{1 \rightarrow j} \int d\tau_1 u_\alpha^*(1) \nabla_1 u_\alpha(1) \int d\tau_j u_\beta^*(j) \nabla_j u_\beta(j)$$

which vanishes since each integral is the expectation value of the linear momentum of an individual electron. Therefore, the

electrons cannot be completely independent of each other, but are governed by the Pauli principle, which demands that the total wave function be antisymmetric with respect to interchange of the coordinates of any pair of electrons. The only possible antisymmetric zero-order wave function which can be constructed from a particular set  $u_o(1)u_v(2)\dots u_p(t)$  belonging to a given configuration is the determinant

$$U = \begin{vmatrix} u_o(1) & \dots & u_o(t) \\ \dots & \dots & \dots \\ u_p(1) & \dots & u_p(t) \end{vmatrix}$$

It may be shown that the diagonal matrix elements for the symmetric function

$$G = \sum_{i,j} g(i,j) = \sum_{i,j} g(j,i)$$

are given by<sup>18</sup>

$$(U|G|U) = \sum_{\alpha > \beta} \iint u_{\alpha}^{*}(1)u_{\beta}^{*}(j)g(i,j)u_{\alpha}(1)u_{\beta}(j)d\tau_1 d\tau_j - \iint u_{\alpha}^{*}(1)u_{\beta}^{*}(j)g(i,j)u_{\beta}(1)u_{\alpha}(j)d\tau_1 d\tau_j \quad (5)$$

where the integrals with positive sign are called direct integrals. If  $g(i,j)$  is independent of spin, then in the zero-order  $n/m_s$  scheme the sum over the spin coordinates implied in the  $\iint$  sign in (5) may be carried out at once. This gives a factor unity on the direct integral and a Kronecker delta  $\delta(m_s^{\alpha}, m_s^{\beta})$  on the exchange integral, so that exchange integrals exist only for electrons with like spin.

Only such diagonal elements taken with respect to various zero-order determinants (wave functions) belonging to the configuration will be needed. The diagonal matrix element of  $G$  taken with respect to one of the zero-order determinants  $U$  is thus



given by (symbolically)

$$(U|\sigma|U) = (1/M) \sum_{\alpha, \beta} (\alpha|p|\alpha)(\beta|p|\beta) - (\alpha|p|\beta)(\beta|p|\alpha)$$

which is expressible in terms of one-electron matrix elements because  $\vec{p}_i \cdot \vec{p}_j$  factorizes. The first terms, being products of linear momentum expectation values, all vanish. Moreover, since  $\vec{p}$  is a vector which anticommutes with the parity operator, the only contributions from the second terms are those for which the pair of indices  $\alpha$  and  $\beta$  refer to  $\ell$ 's differing by one unit. Using the fact that  $(\beta|p|\alpha)$  is the complex conjugate of  $(\alpha|p|\beta)$  one obtains

$$\sigma_{UU} = - (1/M) \sum_{\alpha > \beta} |(\alpha|p|\beta)|^2 = - (h^2/M) \sum_{\alpha > \beta} \left| \int u_{\alpha}^* \nabla u_{\beta} d\tau \right|^2 \quad (6)$$

Therefore the mass correction due to the specific effect is intrinsically negative for each zero-order state. It is not necessarily so for a given Russell-Saunders state of which the zero-order state may be a part. It should be noted that the quantities  $|(\alpha|p|\beta)|^2$  are proportional to the hypothetical probability of optical dipole transition between two one-electron states characterized by the quantum number sets  $\alpha$  and  $\beta$ , and that the two states optically combine only if  $\Delta \ell = \pm 1, \Delta m_{\ell} = \pm 1$  or 0, and  $\Delta m_s = 0$ .

Use of the sum rule. Just as for the electrostatic perturbation, one must determine the shifts in a set of Russell-Saunders states belonging to a given configuration when the specific isotope perturbation is applied. For negligible configuration interaction (i.e., matrix elements of the perturbation connecting different configurations are vanishingly small compared

with the energy separations of the configurations) the Slater method of diagonal sums may be used.<sup>17</sup> A given configuration is now to be considered. There is associated with this configuration a finite set of zero-order determinantal wave functions, all one-electron factors of which have the same  $n$  and  $\ell$ . The number of determinantal wave functions possible is determined by the number of different ways in which the  $m_\ell$ 's and  $m_s$ 's of all the electrons can be arranged, without violation of the Pauli principle. Let the number of such arrangements be  $k$ , and let the wave functions corresponding to these be labelled  $U_1, U_2, \dots, U_k$ . In zero-order, then,  $k$  is the degree of degeneracy for the energy associated with this configuration. Formally, one would then set up the secular equation for these functions as required by degenerate perturbation theory:

$$\begin{vmatrix} (\sigma_{11} - \Delta W) & \sigma_{12} & \dots & \sigma_{1k} \\ \sigma_{21} & (\sigma_{22} - \Delta W) & \dots & \sigma_{2k} \\ \vdots & \vdots & \ddots & \vdots \\ \sigma_{k1} & \sigma_{k2} & \dots & (\sigma_{kk} - \Delta W) \end{vmatrix} = 0$$

The  $\Delta W$  are then the desired specific isotope shifts for the configuration, but a much simpler technique is available for obtaining the energies than that of solving this  $k^{\text{th}}$  degree equation. That technique requires only a knowledge of the zero-order diagonal elements  $\sigma_{11}, \sigma_{22}$ , etc. It makes use of the fact that the element  $\sigma_{mn} = (U_m | \sigma | U_n)$  vanishes unless  $U_m$  and  $U_n$  have the same value of  $\sum m_s$  and the same value of  $\sum m_\ell$ , these quantities being the sums of  $m_s$  and  $m_\ell$  quantum numbers of the one-electron factors comprising  $U_m$  and  $U_n$ . This follows from the spin-independent nature of the perturbation in question. If the rows and

columns of the secular determinant are now labelled by the  $k$  U-functions rearranged in groups having equal  $\sum m_l$  and  $\sum m_s$ , the determinant will factor into a chain of sub-determinants. Each subdeterminant will correspond to a unique  $\sum m_l$ ,  $\sum m_s$  pair and will be of very low degree since only one, two, or three U-functions are generally involved in each of these. A further simplification is afforded by the occurrence of identical roots in several different sub-determinants. That is,

$$\det \left| \begin{array}{c|c|c} A & & \\ \hline & B & \\ \hline & & C \end{array} \right| = \det A \det B \det C \text{ etc.}$$

The reasoning is based on the vector model of the atom. When magnetic effects are neglected, the total orbital angular momentum  $L$  and the total spin angular momentum  $S$ , as well as their sum  $J = L + S$ , are constants of the motion. When the perturbation is applied, the zero-order configuration energy level splits into a number of levels, each characterized by a definite pair of values  $L$  and  $S$ . Moreover, the  $2L + 1$  projections  $M_L$  of  $L$ , and the  $2S + 1$  projections  $M_S$  of  $S$ , also characterize each LS Russell-Saunders level. In the absence of magnetic coupling, therefore, each LS level is  $(2L + 1)(2S + 1)$ -fold degenerate and is associated with  $(2L + 1)(2S + 1)$  functions, each of which may be characterized by an  $M_L M_S$  pair. If the  $\sum m_l$ , and  $\sum m_s$  pair for each U-function is identified with one of the  $M_L M_S$  pairs of the several possible LS levels resulting from the perturbation, it is found that there are exactly as many U-functions as there are  $M_L M_S$  values. Therefore, the energy of each LS level will occur as a root in several of the  $M_L M_S$  sub-determinants. Finally, the sum rule states that the sum of the LS energy roots in any one

$M_L M_S$  sub-determinant is

equal to the sum of zero-order diagonal elements of  $\sigma$  which occur in that sub-determinant. The number of independent algebraic equations thus obtained is usually more than sufficient to determine all the LS roots uniquely in terms of zero-order matrix elements of  $\sigma$ . Determination of the LS wave functions is thus unnecessary.

The helium atom will serve as an example of the use of the method. The configuration is assumed to be  $1s2p$ . The electrons are thus in the state  $n_1 = 1, l_1 = 0, n_2 = 2, l_2 = 1$ , respectively. The notation  $1s^+ 2p^-$  represents the zero-order state:  $n_1 = 1, l_1 = 0, m_{l_1} = 0, m_{s_1} = 1/2, n_2 = 2, l_2 = 1, m_{l_2} = 1, m_{s_2} = -1/2$ .

The following twelve ( $=k$ ) zero-order states (U) occur for the  $1s2p$  configuration:

$1s_0^+ 2p_1^+, 1s_0^+ 2p_0^+, 1s_0^+ 2p_{-1}^+, 1s_0^+ 2p_1^-, 1s_0^+ 2p_0^-, 1s_0^+ 2p_{-1}^-, 1s_0^- 2p_1^+, 1s_0^- 2p_0^+, 1s_0^- 2p_{-1}^+, 1s_0^- 2p_1^-, 1s_0^- 2p_0^-, 1s_0^- 2p_{-1}^-$ . The corresponding  $M_L M_S$  pairs are as follows:

1 1, 0 1, -1 1, 1 0, 0 0, -1 0, 1 0, 0 0, -1 0, 1 -1, 0 -1, and -1 -1.

Now all states in this case must be associated with  $L = 1$  (or P) states since no other total angular momentum can result from the addition of an s and a p electron. Thus, the three possible values of  $M_L$ , i.e., 1, 0, and -1, are the projections of the total angular momentum  $L = 1$ . However, all states with  $M_S = 1$  must be associated with  $S = 1$  (triplet) states, whereas states with  $M_S = 0$  can be associated with  $S = 1$  (triplet) or  $S = 0$  (singlet) states. Three of the  $M_S = 0$  states belong to  $^3P$  ( $L = 1, S = 1$ ) and three belong to  $^1P$  ( $L = 1, S = 0$ ). We see

that the following six  $M_L M_S$  values occur singly: 1 1, 0 1, -1 1, 1 -1, 0 -1, -1 -1. Since each of these corresponds to a one-element determinant, each associated zero-order diagonal matrix element is equal to the  ${}^3P$  energy. Symbolically,

$$(1s_0^+ 2p_1^+) = (1s_0^+ 2p_0^+) = (1s_0^+ 2p_{-1}^+) = (1s_0^- 2p_1^-) = (1s_0^- 2p_0^-) = (1s_0^- 2p_{-1}^-) = ({}^3P)$$

But there are two of each of the pairs 1 0, 0 0, -1 0. Therefore, symbolically,

$$(1s_0^+ 2p_1^-) + (1s_0^- 2p_1^+) = (1s_0^+ 2p_0^-) + (1s_0^- 2p_0^+) = (1s_0^+ 2p_{-1}^-) + (1s_0^- 2p_{-1}^+) \\ = ({}^3P) + ({}^1P) = 0$$

since the zero-order matrix elements vanish for opposed spins. Thus, first  $({}^3P)$  and then  $({}^1P)$  are determined, with  $({}^1P) = -({}^3P)$ . Note that  $({}^3P)$  is negative, according to (6), and that  $({}^1P)$  is therefore positive. Hence, helium-like triplets are lowered and singlets are raised by the specific correction. In this approximation, either  $M_L M_S$  or the quantum numbers  $J = L + S$  and  $M_J = M_L + M_S$  may be associated with the degenerate levels in each multiplet designated by L and S. However, when magnetic interactions are considered, J and  $M_J$  must become the final quantum numbers for the individual levels, each  $SLM_J$  degenerate eigenfunction being a linear combination of  $SLM_L M_S$  eigenfunctions.

One-electron matrix elements. In equation (6) the diagonal matrix elements of the specific effect perturbation are taken with respect to the zero-order antisymmetrized wave functions U belonging to a certain configuration. Each matrix element is a sum of one-electron quantities,  $|(\alpha|p|\beta)|^2$ , which are proportional to the probability of hypothetical radiative transition between state  $\alpha(nl m_l m_s)$  and  $\beta(n' l' m_l' m_s')$ . Since the one-electron

functions are products of radial and angle functions, and

$$\Delta m_s = 0,$$

$$|(\alpha | p | \beta)|^2 = C(n\ell, n'\ell') D(\ell, m_\ell, \ell', m_{\ell}') \delta(m_s, m_{s}')$$

where C depends on the integration of radial functions, and D on angle integrations which are known for hydrogenic transitions.

Thus, for  $m_s = m_s'$ , the terms in equation (6) are given by<sup>19</sup>

$$\begin{aligned} |(n\ell m, p | n'\ell-1, m_{\ell} \pm 1)|^2 &= C(n\ell, n'\ell-1) \left\{ (1/2) (\ell \mp m_{\ell}) (\ell \mp m_{\ell} - 1) \right\} \\ |(n\ell m, p | n'\ell-1, m_{\ell})|^2 &= C(n\ell, n'\ell-1) \left\{ \ell^2 - m_{\ell}^2 \right\} \end{aligned} \quad (7)$$

All possible cases are covered by (7) due to the selection rules.

The factor C must be calculated in any given case and has been shown to be given by<sup>4</sup>

$$C(n\ell, n'\ell-1) = \frac{n^2}{4\ell^2-1} \left\{ \int_0^\infty R_{n\ell} \frac{d}{dr} R_{n'\ell-1} - \frac{(\ell-1)}{r} R_{n'\ell-1} r^2 dr \right\}^2 \quad (8)$$

where  $R_{n\ell}$  is the Hartree radial function for the  $n\ell$  orbit, so

normalized that  $\int_0^\infty R_n^2 r^2 dr = 1$ . It is of interest to note

that the curly bracket in the expression for C may be given by<sup>20</sup>

$$\left\{ \right\} = \frac{M}{n^2} \left[ (W_{n'\ell-1} - W_{n\ell}) \int_0^\infty R_{n\ell} R_{n'\ell-1} r^3 dr - \int_0^\infty (v_{n'\ell-1} - v_{n\ell}) R_{n\ell} R_{n'\ell-1} r^3 dr \right] \quad (9)$$

where  $W_{n\ell}$  is the energy of an electron in the  $n\ell$  orbit and  $v_{n\ell}$  is the corresponding effective central field. If the approximation is made that the  $v$ 's are the same and that the energies  $W_{n\ell}$  and  $W_{n'\ell-1}$  are known, the expression for C and thus the specific isotope shifts for the configuration would depend only on the integral  $\int R_{n\ell} R_{n'\ell-1} r^3 dr$ , which is essentially the dipole moment radial integral for a transition between an  $n\ell$  state and an  $n'\ell-1$  state.

## II. SPECIFIC ISOTOPE SHIFT PARAMETERS FOR OXYGEN

In the application of the theory, the quantities  $C(n\ell, n'\ell')$  are treated as unevaluated parameters, because of the unavailability of excited state Hartree wave functions. For neutral oxygen, a configuration consists of eight  $n\ell$  values, seven for the ionic core and one for the optical electron:  $1s^2 2s^2 2p^3 n\ell$ . The core contribution is an additive constant for all states and can be separately considered. All three Russell-Saunders states of the core,  $^4S$ ,  $^2D$ , and  $^2P$ , upon each of which an entire energy level system is built when the optical electron is added to it, have the same specific shift. The reason for this is that the 2p-electrons combine (in the sense of equation (7)) only with the s-electrons and not with each other. Therefore, the core contribution is independent of the  $m_\ell$  and  $m_s$  values of the 2p-electrons, and is given by

$$\Delta W(\text{core}) = -3aC(2p, 1s) - 3aC(2p, 2s)$$

where  $a = (M_{18} - M_{16})/M_{18}M_{16}$ ,  $M_{18}$  being the mass of the  $O^{18}$  nucleus and  $M_{16}$  the mass of the  $O^{16}$  nucleus. In the following discussion, this contribution is disregarded since only the relative shift between two levels is measurable.

The addition to the core of an optical electron is now considered. It can immediately be seen that the addition of an np-electron gives the same specific shift for all Russell-Saunders terms in all three systems arising from the configuration  $1s^2 2s^2 2p^3 np$ . As in the case of the core, the np-electron combines only with the s-electrons, and the shift, which is independent of the  $m_\ell$  and  $m_s$  values of the p-electrons, is



therefore

$$\Delta W(\text{all } np \text{ terms}) = -aC(np, 1s) - aC(np, 2s)$$

An s-electron added to the core, however, gives rise to the following Russell-Saunders terms:  $^5S$ ,  $^3S$ ,  $^3D$ ,  $^1D$ ,  $^3P$ , and  $^1P$ .

Each of these may have different shifts and a detailed analysis is necessary. The procedure, formally identical to that followed for the electrostatic perturbation, consists of setting up a table with  $\sum m_s = M_S$  values along the top and  $\sum m_l = M_L$  values along the side. All possible combinations of one-electron quantum states having a particular  $M_L$  and  $M_S$  pair are written in the corresponding box in the table. Also in that box are written the Russell-Saunders terms which have components there. This is illustrated in Table II. In those boxes having one zero-order state and one Russell-Saunders term, the diagonal matrix element formed with the zero-order state (see equation (6)) is equal to the energy of the Russell-Saunders term. In boxes with several zero-order states, the sum of the zero-order diagonal matrix elements is equal to the sum of energies of the corresponding set of Russell-Saunders terms. This illustrates the use of the diagonal sum rule. Only that quadrant of the table corresponding to positive  $M_L$  and  $M_S$  values is needed. Other quadrants give redundant information and may be used as a check. The seven boxes shown in Table II provide seven algebraic equations for the six unknowns. The total number of Russell-Saunders states labelled by  $M_L M_S$  (or by  $J M_J$ ) is 40 and the total number of zero-order states is, correspondingly, 40.



TABLE II

CLASSIFICATION OF EIGENFUNCTIONS OF THE CONFIGURATION  $2p^3ns$   
FOR USE OF ENERGY SUM RULE

$M_S \rightarrow$	2	1	0
$M_L$			
$\downarrow$			
2		$(p_1^+ p_0^+ p_1^- s_0^+)$ $3D$	$(p_1^+ p_0^+ p_1^- s_0^-), (p_1^- p_0^- p_1^+ s_0^+)$ $3D, 1D$
1		$(p_1^+ p_0^+ p_0^- s_0^+),$ $(p_1^+ p_1^+ p_1^- s_0^+)$ $3D, 3P$	$(p_1^+ p_0^+ p_0^- s_0^-), (p_1^- p_0^- p_0^+ s_0^+),$ $(p_1^+ p_1^+ p_1^- s_0^-), (p_1^- p_1^- p_1^+ s_0^+)$ $3D, 1D, 3P, 1P$
0	$(p_1^+ p_0^+ p_1^+ s_0^+)$ $5S$	$(p_1^+ p_1^+ p_0^- s_0^+),$ $(p_0^+ p_1^+ p_1^- s_0^+),$ $(p_0^+ p_1^+ p_1^- s_0^-),$ $(p_1^+ p_0^+ p_1^+ s_0^-)$ $3D, 3P,$ $3S, 5S$	$(p_1^+ p_1^+ p_0^- s_0^-), (p_1^- p_1^- p_0^+ s_0^+),$ $(p_0^+ p_1^+ p_1^- s_0^-), (p_0^- p_1^- p_1^+ s_0^+),$ $(p_0^+ p_1^+ p_1^- s_0^-), (p_0^- p_1^- p_1^+ s_0^+)$ $5S, 3S, 3D, 1D,$ $3P, 1P$

(<sup>4</sup>S) System:(<sup>2</sup>D) System:(<sup>2</sup>P) System:

$$\Delta W(^5S) = -3aC(2p, ns) \quad \Delta W(^3D) = -2aC(2p, ns) \quad \Delta W(^3P) = -2aC(2p, ns)$$

$$\Delta W(^3S) = aC(2p, ns) \quad \Delta W(^1D) = 0 \quad \Delta W(^1P) = 0$$

### III. COMPARISON OF THEORETICAL PREDICTIONS WITH EXPERIMENTAL RESULTS IN OXYGEN

An immediately verifiable prediction of the theory is that all levels arising from the addition to the core of a 3p electron must have the same specific shift. Therefore, the relative specific shift between any two of these levels must vanish and the total shift should be given by the relative normal effect alone. The measured relative shift between two 3p levels may be obtained if both levels are connected with a third common level by two lines whose shifts have been measured. As may be seen in the energy level diagram, Figure 9, five 3p levels,  $3p^3P$ ,  $3p^1D$ ,  $3p^3D$ ,  $3p^1D$ , and  $3p^1F$ , are interconnected through the lines  $\lambda 7157$ ,  $\lambda 8820$ ,  $\lambda 3823$ ,  $\lambda 8222$ ,  $\lambda 7995$ ,  $\lambda 3955$ , and  $\lambda 7476$ . Table III shows how the observed relative shift compares with the expected (normal) shift in five pairs of 3p levels. Corresponding pairs of connecting lines are indicated, with plus or minus signs denoting whether the observed shifts in the lines have been added or subtracted to obtain the relative shift in the 3p levels. Taken from Table I, the numbers have been rounded off in accordance with the experimental accuracy with which they have been obtained. Except for the shift involving  $\lambda 7476$ , the comparison is quite favorable.

TABLE III  
COMPARISON OF OBSERVED AND NORMAL RELATIVE SHIFTS  
IN PAIRS OF 3p LEVELS

Level Pair	Connecting Lines	Observed Shift ( $\text{cm}^{-1}$ )	Normal Shift ( $\text{cm}^{-1}$ )
$3p' \ ^1F - 3p' \ ^1D$	7157 - 8820	< 0.01	0.01
$3p' \ ^3D - 3p'' \ ^3D$	3823 - 8222	0.06	0.05
$3p \ ^3P - 3p' \ ^3D$	8222 + 7995	0.07	0.10
$3p \ ^3P - 3p'' \ ^3D$	3823 + 7995	0.12	0.15
$3p \ ^3P - 3p'' \ ^3D$	3955 + 7476	< 0.1	0.15

The shifts in individual 3s and 3p levels are given in terms of the parameters  $aC(2p,3s)$  and  $a[C(3p,1s) + C(3p,2s)]$  respectively. These may be empirically determined from two measured transitions between 3s and 3p levels. The lines  $\lambda 7772(3s^5S - 3p^5P)$  and  $\lambda 8820(3s^1D - 3p^1F)$  are used since their shifts are known with relatively high precision. Moreover, the quintet levels are not likely to be perturbed by configuration interactions. The specific shift in  $\lambda 7772$  is given by  $-3aC(2p,3s) + a[C(3p,1s) + C(3p,2s)]$  and the specific shift in  $\lambda 8820$  is given by  $a[C(3p,1s) + C(3p,2s)]$ . The measured specific shift in  $\lambda 7772$  is  $\Delta v_{sp}(7772) = 0.013 \rightarrow 0.019 \text{ cm}^{-1}$  and that in  $\lambda 8820$  is  $\Delta v_{sp}(8820) = 0.064 \rightarrow 0.068 \text{ cm}^{-1}$ . From these values the parameters of interest are obtained:

$$aC(2p,3s) = 0.015 \rightarrow 0.018 \text{ cm}^{-1}$$

$$a[C(3p,1s) + C(3p,2s)] = 0.064 \rightarrow 0.068 \text{ cm}^{-1}$$

Table IV lists the specific shift parameters necessary for the calculation of the shifts in several lines. The comparison between empirically predicted and observed shifts affords some test of the theory. The overall comparison, including the cases of the relative shifts between 3p levels, seems to show a general agreement with the theory, at least regarding sign and order of magnitude. The greatest discrepancy is found in the shift for  $\lambda 7476$ , which not only has the wrong sign with respect to theoretical expectation, but fails to be energetically consistent with the shifts of  $\lambda \lambda 3823$ , 7995, and 3955, which form a closed quadrilateral with  $\lambda 7476$ . Moreover,  $\lambda 7476$  is a multiplet with several components, but only one was found. One conceivable explanation would be that the line has been incorrectly classified.

TABLE IV

## PREDICTED VERSUS OBSERVED SPECIFIC SHIFTS\*

Specific shift for all  $3p$ ,  $3p'$ , and  $3p''$  states:  $-a[C(3p,1s) + C(3p,2s)] = -0.064 \rightarrow -0.068 \text{ cm}^{-1}$

" " "  $3s$  triplet:  $aC(2p,3s) = 0.015 \rightarrow 0.018 \text{ cm}^{-1}$

" " "  $3s'$  or  $3s''$  triplet:  $-2aC(2p,3s) = -0.030 \rightarrow -0.036 \text{ cm}^{-1}$

" " "  $3s'$  or  $3s''$  singlet: zero  $\text{cm}^{-1}$

Wave-length	Transition	Predicted Shift ( $\text{cm}^{-1}$ )	Observed Shift ( $\text{cm}^{-1}$ )
8446	$3s \ ^3S - 3p \ ^3P$	$aC(2p,3s) + a[C(3p,1s) + C(3p,2s)] = 0.079 \rightarrow 0.086$	$0.08 \rightarrow 0.10$
3955	$3p \ ^3P - 3s'' \ ^3P$	$-a[C(3p,1s) + C(3p,2s)] + 2aC(2p,3s) = -0.028 \rightarrow -0.038$	$0 \rightarrow -0.20$
8222	$3s' \ ^3D - 3p' \ ^3P$	$-2aC(2p,3s) + a[C(3p,1s) + C(3p,2s)] = 0.028 \rightarrow 0.038$	$0.034 \rightarrow 0.040$
3823	$3s' \ ^3D - 3p'' \ ^3D$	$-2aC(2p,3s) + a[C(3p,1s) + C(3p,2s)] = 0.028 \rightarrow 0.038$	$0.03 \rightarrow 0.05$
7157	$3s' \ ^1D - 3p' \ ^1D$	$a[C(3p,1s) + C(3p,2s)] = 0.064 \rightarrow 0.068$	$0.05 \rightarrow 0.07$
7995	$3p \ ^3P - 3s' \ ^3D$	$-a[C(3p,1s) + C(3p,2s)] + 2aC(2p,3s) = -0.028 \rightarrow -0.038$	$-0.06 \rightarrow -0.07$
7476	$3s'' \ ^3P - 3p'' \ ^3D$	$-2aC(2p,3s) + a[C(3p,1s) + C(3p,2s)] = 0.028 \rightarrow 0.038$	$-0.04 \rightarrow -0.06$

\*Parameters are empirically determined from measured shifts in  $\lambda 7772$  and  $\lambda 8820$ .

The extremely large observed shifts in  $\lambda 4233$  and  $\lambda 2884$  may be accounted for by assigning a large specific shift to the common upper level,  $3d' \ ^3P$ . Assuming all the residual shifts to be due to the specific effect, one may use the measured shifts in the lines  $\lambda 4368 (3s \ ^3S - 4p \ ^3P)$  and  $\lambda 4233 (4p \ ^3P - 3d' \ ^3P)$  to determine the specific effect in the  $3d' \ ^3P$  level, which is given by  $\Delta W_{sp}(3d' \ ^3P) = -0.43 \rightarrow -0.48 \text{ cm}^{-1}$ . The unexpected size of this shift seems to indicate that the above form of the theory may not be satisfactory for this level. R. E. Trees<sup>21</sup> has suggested that a considerable configuration interaction may be occurring between  $3d' \ ^3P$  and  $2s2p^5 \ ^3P$ , in which part of the large shift expected in the latter may be shared by the former. The theory outlined above has not taken into account possible configuration interactions, the inclusion of which involves additional parameters and makes the calculation considerably more complex. Such configuration interaction effects might account in part for the slight discrepancy between predicted and observed shifts in  $\lambda 7995$ .

Where it has been possible to compare shifts in the components within a multiplet, such as in  $\lambda 8222$ ,  $\lambda 7772$ , and  $\lambda 8446$ , the shifts are found to be the same within experimental accuracy. This is expected of transitions between Russell-Saunders levels, where the shifts are independent of J-values. Most of the oxygen levels should be characterizable by LS-coupling since the fine structure splittings are very small.

IV. TRANSITION PROBABILITY AND  $f$  VALUE

It is of interest to make use of the formal relationship of the specific effect parameters to certain radiation theory integrals, as has been suggested elsewhere.<sup>5</sup> With several gross assumptions, a transition probability and an  $f$ -value for the oxygen  $\lambda 1306(2p^4 \ ^3P - 2p^3 3s \ ^3S)$  resonance triplet may be calculated with the empirically determined parameter (equation (8))

$$C(2p, 3s) = (n^2/3) \left\{ \int_0^\infty R_{2p} \frac{dR_{3s}}{dr} r^2 dr \right\}^2$$

The formal relationship required is (equation (9))

$$\left\{ \right\}^2 \approx (m^2/n^4) (W_{3s} - W_{2p})^2 (r)^2$$

$W_{3s}$  and  $W_{2p}$  are the approximate energies required to remove a  $3s$  electron and a  $2p$  electron respectively, and  $(r)$  is the dipole moment radial integral

$$(r) = \int_0^\infty R_{2p} R_{3s} r^3 dr$$

The approximation has been made that the  $3s$  and  $2p$  electrons move in the same central field. Thus, in equation (9)  $v_{2p}$  and  $v_{3s}$  are equal. The validity of this assumption can only be tested by an actual calculation. Having  $(r)$ , one may then find the one-electron transition strength<sup>22</sup>

$$s^2 = (1/3)e^2 (r)^2$$

where  $e$  is the electronic charge. The total strength of the transition,  $S^2(2p^4 \ ^3P - 2p^3 3s \ ^3S)$ , is given in terms of  $s^2$  by<sup>23</sup>

$$S^2 = 12s^2 = 4e^2(r)^2$$

From this one may find the spontaneous transition probability<sup>24</sup> for emission of the  $\lambda 1306$  multiplet:

$$A = (64\pi^4 \nu^3 / 3h) S^2$$

where  $\nu$  is the wave number of the transition. One may also find the f value or oscillator strength for  $\lambda 1306$  by<sup>24</sup>

$$f = (8\pi^2 m \nu c / 3e^2 h) S^2$$

Now  $(W_{3s} - W_{2p})$  is the difference in average energies of the terms in the 3s and 2p configurations. From an energy level table<sup>25</sup>  $(W_{3s} - W_{2p})$  is found to be approximately  $94,700 \text{ cm}^{-1}$ , or  $1.88 \times 10^{-11} \text{ erg}$ . If  $aC(2p, 3s)$  is taken to be  $0.0165 \text{ cm}^{-1}$ , it follows for  $a = 4.16 \times 10^{21} \text{ g}^{-1}$  that  $C(2p, 3s) = 3.97 \times 10^{-24} \text{ g} \cdot \text{cm}^{-1}$ , or  $7.88 \times 10^{-40} \text{ g-erg}$ .

Thus,

$$(r)^2 = 3h^2 C(2p, 3s) / m^2 (W_{3s} - W_{2p})^2 = 8.98 \times 10^{-18} \text{ cm}^2$$

or,  $(r) = 0.30 \times 10^{-8} \text{ cm}$ . That this is a reasonable value follows from the fact that  $(r)$  should be of the order of an atomic unit of length, which is about  $0.5 \times 10^{-8} \text{ cm}$ .

For the  $\lambda 1306$  multiplet, finally,  $A = 1.16 \times 10^9 \text{ sec}^{-1}$ , corresponding to a reasonable lifetime of about  $10^{-9}$  seconds for the multiplet. Moreover,  $f = 0.298$ , which is reasonable for the effective number of electrons.



## V. COMPARISON OF OXYGEN WITH NITROGEN

Since isotope shift measurements have been made on nitrogen,<sup>26</sup> it is possible to compare empirically determined parameters for nitrogen with corresponding parameters for oxygen. The parameters of interest are those for 3s and 3p levels. With the same diagonal sum method used for oxygen it is found that the needed shifts are as follows:

$$\Delta W(3s^4P) = -2a_N C_N(2p, 3s)$$

$$\Delta W(3s^2P) = a_N C_N(2p, 3s)$$

$$\Delta W(\text{all } 3p \text{ states}) = -a_N [C_N(3p, 1s) + C_N(3p, 2s)]$$

where  $a_N = (M_{15} - M_{14})/M_{15}M_{14}$ ,  $M_{14}$  being the mass of the  $N^{14}$  nucleus and  $M_{15}$  the mass of the  $N^{15}$  nucleus.

For the multiplet  $\lambda 8568\text{-}8656(3s^2P - 3p^2P)$ , the specific shift is found to be  $0.038 \rightarrow 0.049 \text{ cm}^{-1}$ . In the group  $\lambda 8703\text{-}8719(3s^4P - 3p^4D)$  the specific shift is  $-0.090 \text{ cm}^{-1}$  with high precision. The group  $\lambda 8185\text{-}8243(3s^4P - 3p^4P)$  has the specific shift  $-0.08 \rightarrow -0.09 \text{ cm}^{-1}$ , and the group  $\lambda 7424\text{-}7469(3s^4P - 3p^4S)$  has the specific shift  $-0.08 \rightarrow -0.10 \text{ cm}^{-1}$ . In terms of theoretical parameters, the shift in the transition  $(3s^2P - 3p^2P)$  is given by  $a_N C_N(2p, 3s) + a_N [C_N(3p, 1s) + C_N(3p, 2s)]$ . The specific shift with the least spread in the other three groups is that found in the transition  $(3s^4P - 3p^4D)$ , and is given theoretically by  $-2a_N C_N(2p, 3s) + a_N [C_N(3p, 1s) + C_N(3p, 2s)]$ . Thus, one may obtain the parameters

$$a_N C_N(2p, 3s) = 0.043 \rightarrow 0.046 \text{ cm}^{-1}$$

and

$$a_N [C_N(3p, 1s) + C_N(3p, 2s)] = 0 \text{ cm}^{-1}$$

In contrast, the corresponding parameters for oxygen are

$$a_O C_O(2p, 3s) = 0.015 \rightarrow 0.018 \text{ cm}^{-1}$$

and

$$a_O [C_O(3p, 1s) + C_O(3p, 2s)] = 0.064 \rightarrow 0.068 \text{ cm}^{-1}$$

Since the ratio of the factors  $a_O/a_N$  is about 3/2, the value of  $C_N(2p, 3s)$  is some 9/2 that of  $C_O(2p, 3s)$ . On the other hand, the sum  $[C_N(3p, 1s) + C_N(3p, 2s)]$  is vanishingly small for nitrogen, but  $[C_O(3p, 1s) + C_O(3p, 2s)]$  is appreciable for oxygen. A discrepancy is apparent, for it may be expected that all parameters should have the same general trend, i.e., get larger or smaller, from one atom to the next. However, all the above nitrogen multiplets occurring as transitions between different 3p levels and the same 3s level do have the same specific shift, within experimental error, as would be demanded by the theory.

## CHAPTER V

### NEW FINE STRUCTURE

The thorough work of Edlén<sup>27</sup> on the atomic spectrum of oxygen has required no essential revisions. There are, however, many levels of O I whose spin-orbit splittings are so small that the associated multiplet lines have remained unresolved or only partially resolved, and augmentations of Edlén's data were to be expected as greater resolution became available. During the study of isotope shifts in O I discussed above, new fine structure was uncovered in the lines  $\lambda 8446$ ,  $\lambda 4368$ , and  $\lambda 2884$ .

## I. EXPERIMENTAL PROCEDURE

The technique used for the fine structure was identical to that used for isotope shifts, except that relative intensities were required in addition for the fine structure analysis.

Plate calibrations were made for each of the three wavelengths with time exposures of the same order of duration as those of the spectral exposures to minimize reciprocity failure. For  $\lambda 2884$  a calibration made with a step-weakeners agreed well with the corresponding time calibration. Silvered interferometer plates were used for  $\lambda 8446$  and  $\lambda 4368$ , and aluminized plates for  $\lambda 2884$ . The density contours of the interferometer patterns were reproduced, as in the case of the isotope shifts, by a Zeiss microphotometer connected to a Speedomax Leeds and Northrup recorder. The fine structure splittings were determined by measuring the relative positions of pattern maxima and using MacNair's method of calculating the displacements in terms of fractions of an order.<sup>14</sup>

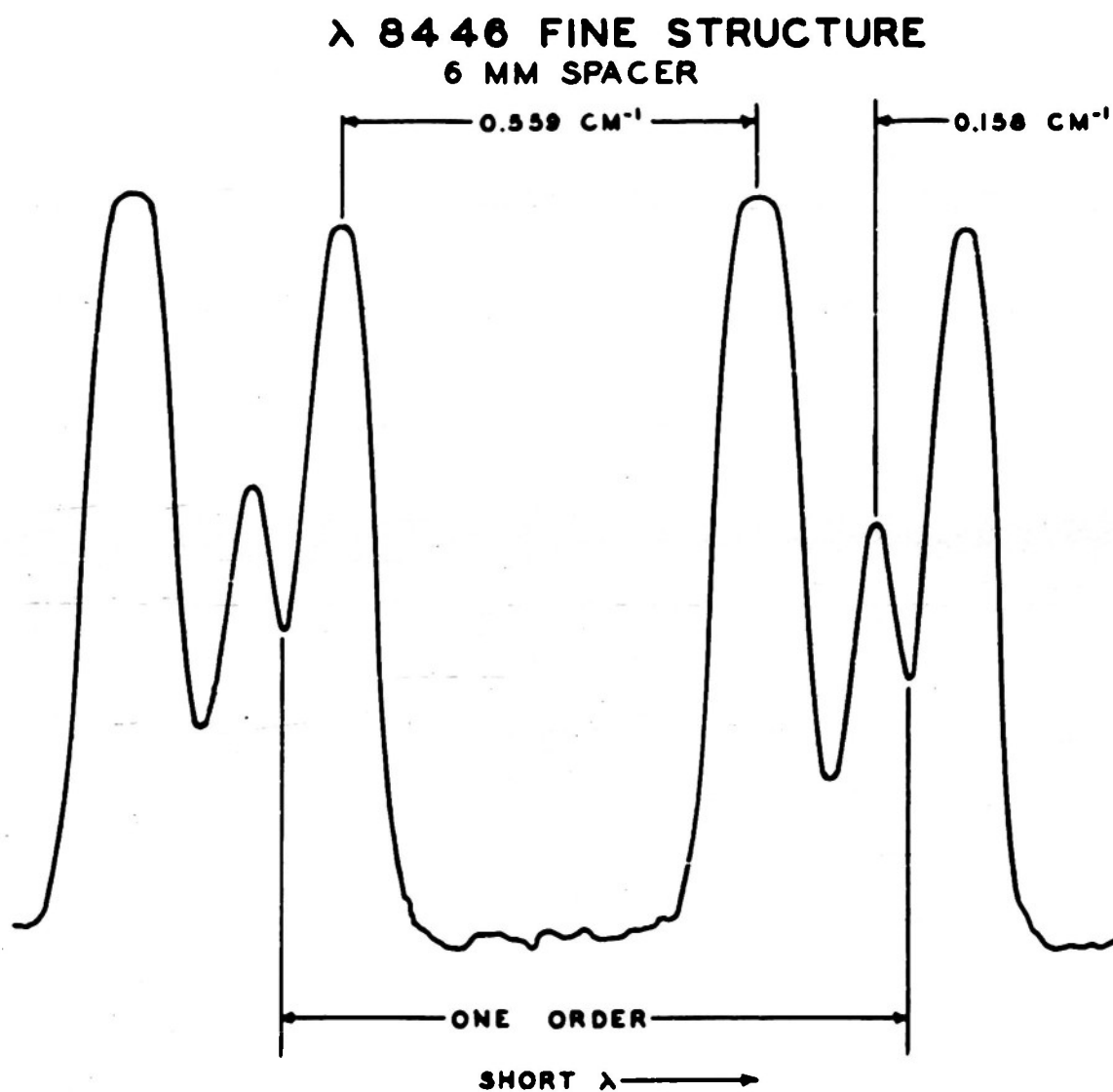
$\lambda 8446$ . Two spacers, 5mm and 6mm, were used to obtain interferometer patterns which show all three fine structure components clearly separated, as Figures 6 and 7 show. This triplet was so strong that a fine-grained IV-N plate could be used, but the contrast for this type of plate is too great for photometric purposes. On the other hand, a fresh I-N plate with low contrast would be blackened in a few seconds, which was too short a time for accurate time exposure calibration. An old I-N plate was found to have the proper contrast and was sufficiently slow to allow an exposure time of several minutes. An infrared lamp was used for the calibration. The background of the plate used was quite clean, as

Figure 10 indicates. Because of the overlapping wings of the two strongest components, the weakest is spuriously shifted toward the nearer of its neighbors, i.e., toward the second strongest component of the 6 mm pattern. The 5 mm spacer, on the other hand, places the weakest component closer to the strongest component. Therefore, the value for the displacement of the weakest component from the strongest, given in Table V as  $^3P_2 - ^3P_0$ , was obtained as a weighted average of the values obtained with the 5 mm and 6mm spacers. The weights were taken to be proportional to the "nearness" of the weakest component to the exact midpoint of the interval between the two strongest components. With the notation  $\Delta_{21} \equiv ^3P_2 - ^3P_1$  denoting the interval between the two strongest components, and  $\Delta_{20} \equiv ^3P_2 - ^3P_0$  denoting the interval between the strongest and weakest components, the weight ascribed to the value  $^3P_2 - ^3P_0$  obtained from either trace was taken to be

$$w = 1 - |\Delta_{20} - (1/2)\Delta_{21}| / (1/2)\Delta_{21}$$

$\lambda 2884$ . A 4 mm spacer placed the weaker component of this doublet almost exactly midway between orders. About 30 minutes were required for an exposure on a II-0 plate. A hydrogen arc lamp continuum was used for the calibration. Molecular band background was present.

$\lambda 4368$ . The strength of this doublet (incompletely resolved triplet) was great enough to allow the use of a very fine grain IV-0 plate for the splitting determination, a II-0 plate being somewhat grainier for  $\lambda 4368$  than a I-N for  $\lambda 8446$ . However, more proper contrast was provided by II-0 plates, and two of these were used for the relative intensity measurements; both plates gave the same relative intensity ratio. About 90 seconds were

**FIGURE 10**

**FABRY-PEROT FRINGES SHOWING ALL THREE  
COMPONENTS OF  $\lambda$ 8446**

TABLE V  
NEW FINE STRUCTURE IN NEUTRAL ATOMIC OXYGEN

Wavelength	Transition	Splittings ( $\text{cm}^{-1}$ )	Intensity Ratio of Components
8446	$3s\ ^3S_1 - 3p\ ^3P_{210}$	$^3P_2 - ^3P_1 = 0.559(\pm 0.003)$ $^3P_2 - ^3P_0 = -0.158(\pm 0.002)$	1:0.64:0.30
2884	$3p\ ^3P_{21} - 3d\ ^3P_2$	$^3P_2 - ^3P_1 = 0.558(\pm 0.002)$	1:0.66
4368	$3s\ ^3S_1 - 4p\ ^3P_{210}$	$^3P_{21} - ^3P_0 = -0.300(\pm 0.001)$	1:0.26

required for an exposure on a II-0 plate, and 20 minutes for a IV-0 plate.

For  $\lambda 2884$  and  $\lambda 4368$ , densitometer traces with both small and large lateral magnifications were made, the smaller having about 5 cm, the larger about 13 cm, between orders. For both lines, the larger magnifications were found to give smaller data dispersions.



## II. RESULTS

Table V shows the splittings and relative intensities for the three transitions studied. The figures in parentheses are probable errors. The displacements in wave numbers were obtained with the relationship

$$\Delta v = \Delta n / 2d \text{ cm}^{-1}$$

where  $\Delta n$  is the displacement in fractions of an order, and  $d$  is the spacer size. Ten orders were used to obtain data for  $\lambda 8446$ , twelve for  $\lambda 2884$ , and twelve for  $\lambda 4368$ . Relative intensities within a multiplet were obtained by drawing a smooth curve through each set of peaks and obtaining the average of several determinations of relative intensities in different places along the nearly flat central portions of these curves.<sup>28</sup> The heights, converted to intensities by means of the calibration, were taken with respect to the background level, which was very uniform over the entire photographic plate in all cases. The values of relative intensity given in Table V probably should be considered as upper limits because of the non-vanishing instrumental background characteristic of interferometer fringes.<sup>28</sup> The effect of such background may be small but is difficult to evaluate. However, the error in intensity measurements is estimated to be 15%. The values  $^3P_2 - ^3P_1$  for  $\lambda 8446$  and  $^3P_2 - ^3P_1$  for  $\lambda 2884$  should be (and are found to be) equal since the same two fine structure levels are involved, as shown by Figure 11.

### III. DISCUSSION

The complete anomalous structure of the  $3p\ ^3P$  level was inferred from its combination with  $3s\ ^3D$  by Edlén with the intensity sum rule. This rule states that for any Russell-Saunders multiplet the sum of the intensities of the lines having a given initial (final) level is proportional to the statistical weight,  $2J + 1$ , of that initial (final) level. The complex multiplet corresponding to the above transition is  $\lambda 7982-95$ . Although the doublet structure of  $\lambda 7982.41$ , which ends on  $^3P_{20}$ , was not resolved directly by Edlén, he determined the splitting  $^3P_2 - ^3P_0$  (giving it as  $0.16\text{ cm}^{-1}$ ) by noting that the splitting of the line pair  $^3P_{0,1} - ^3D_1$  was measurably greater than that of the line pair  $^3P_{1,2} - ^3D_2$ . There have remained, however, about a dozen lines involving the  $3p\ ^3P$  level which are incompletely resolved with respect to this level and which are expected to have splittings based on the known structure of  $3p\ ^3P$ . Two of these are  $\lambda 8446.35$  and  $\lambda 2883.78$ , the former wavelength determined by Edlén, the latter by Runge and Paschen.<sup>29</sup> The complete resolution of the  $\lambda 8446$  triplet as well as of the  $\lambda 2884$  doublet, confirms the structure of  $3p\ ^3P$  established by Edlén. The relative intensity ratio found for the three components of  $\lambda 8446$ , 1: 0.64: 0.30, was used to associate J-values of  $3p\ ^3P$  with individual components. That is,  $J = 2$  is associated with the strongest,  $J = 1$  with the second strongest, and  $J = 0$  with the weakest. This ratio deviates slightly from the theoretical ratio expected for pure Russell-Saunders coupling, i.e., 1:0.60:0.20, since the statistical weights of the  $J = 2$ , 1, and 0 levels are 5, 3, and 1, respectively. The discrepancy may be due to an error in the

relative intensity measurement since it is well known that instrumental background between orders in interferometer patterns can sometimes increase the apparent relative intensity of weak components by an order of magnitude.<sup>28</sup> One may examine the effect on  $\lambda 2884$  of band background, which is definitely present in addition to the instrumental background. In this case the relative intensity ratio of the two components, ending on  $J = 2$  and  $J = 1$  of  $3p\ ^3P$ , is found to be 1:0.66, respectively, whereas the theoretical ratio is 1:0.60. The corresponding ratio found for  $\lambda 8446$ , 1:0.64, is negligibly different. There is a distinct possibility, then, that the deviation of the  $\lambda 8446$  relative intensity ratio from the theoretically expected ratio may be due at least in part to a perturbation effect. Edlén has shown that the entire  $np\ ^3P$  series is perturbed by  $3p'\ ^3P$  in the displaced  $^2D$  system. This level, expected at a position above the ionization limit of the normal  $^4S$  system, is missing due to a strong auto-ionization effect in which the  $3p'\ ^3P$  level interacts with the continuum above the  $np\ ^3P$  series limit.

The structure found for  $\lambda 4368$  is interesting since this line originates on  $4p\ ^3P$  of the  $np\ ^3P$  perturbed series. Since only two components were resolvable, there remained the problem of deciding which two of the three levels  $J = 0, 1, 2$  coincide. The choice made was based on the relative intensity ratio, found to be 1:0.26. The three possibilities of coincidence were as follows:  $J = 0, 1$ ;  $J = 0, 2$ ; and  $J = 1, 2$ . These would result in the relative intensity ratios 1:0.80, 1:0.50, and 1:0.125, respectively. The last possibility is most reasonable, since the presence of instrumental background would require that 0.26 be

considered an upper limit. Figure 11 indicates the inferred structure of  $4p\ ^3P$ , which is anomalous. It is to be expected that higher terms of the  $np\ ^3P$  series, lying closer to the perturbing level, should be even more distorted.

The same kind of perturbation is probably responsible for the very appearance of lines such as  $\lambda 7932$ ,  $\lambda 2884$ ,  $\lambda 3823$ , and  $\lambda 3955$ , and others which connect terms of the different systems,  $^4S$ ,  $^2D$ , and  $^2P$ . These lines end on levels similar in character to levels which are in the same system as the initial levels but which vanish because of autoionization. Such transitions are otherwise forbidden.<sup>30</sup>

## FINE STRUCTURE TRANSITIONS

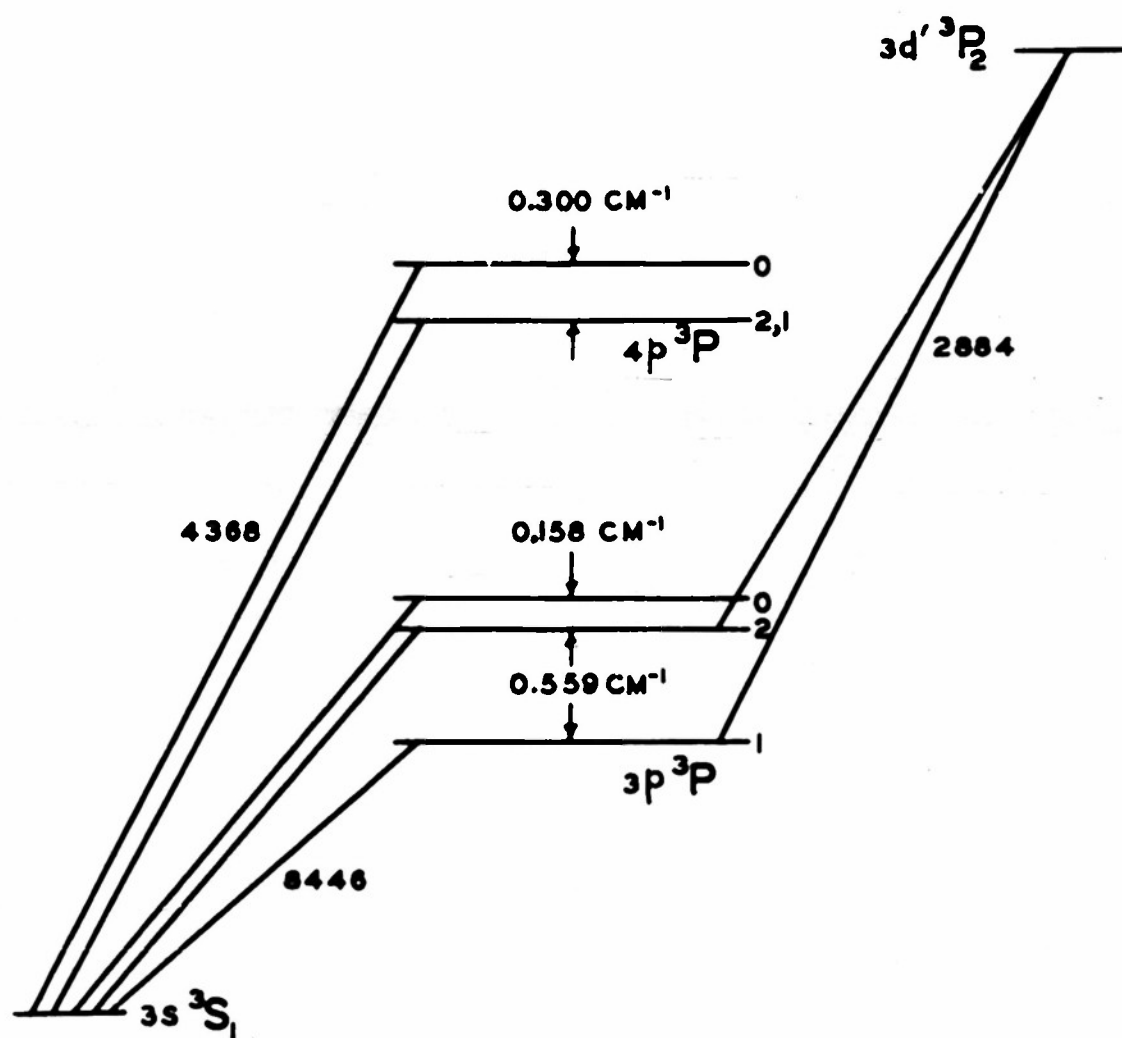


FIGURE 11

ENERGY LEVEL DIAGRAM FOR O I SHOWING FINE STRUCTURE  
TRANSITIONS STUDIED AND THE DEDUCED STRUCTURES  
OF  $3p\ ^3P_{210}$  AND  $4p\ ^3P_{210}$

## REFERENCES

- 1 E. W. Foster, Repts. Prog. Phys. 14, 288 (1951); J. R. McNally, Jr., Am. J. Phys. 20, 152 (1952).
- 2 H. C. Urey, F. G. Brickwedde, and G. M. Murphy, Phys. Rev. 40, 1 (1932).
- 3 D. S. Hughes and Carl Eckart, Phys. Rev. 36, 694 (1930).
- 4 J. H. Bartlett, Jr., and J. J. Gibbons, Phys. Rev. 44, 538 (1933).
- 5 John P. Vinti, Phys. Rev. 56, 1120 (1939).
- 6 W. Opechowski and D. A. DeVries, Physica 6, 913 (1939); John P. Vinti, Phys. Rev. 58, 879 (1940).
- 7 Mark Fred et al., Phys. Rev. 82, 406 (1951).
- 8 James H. Bartlett, Jr., Nature 128, 408 (1931); M. F. Crawford and A. L. Schawlow, Phys. Rev. 76, 1310 (1949).
- 9 M. F. Crawford et al., Can. J. Research A28, 138 (1950).
- 10 The work reported herein on isotope shifts has been published in the following paper: Lee W. Parker and John R. Holmes, Journ. Opt. Soc. Am. 43, 103 (1953).
- 11 The work reported herein on fine structure has been published in the following paper: Lee W. Parker and John R. Holmes, Phys. Rev. 90, 142 (1953).
- 12 S. Tolansky, High Resolution Spectroscopy (New York: Pitman Corp., 1947), pp. 145 ff.
- 13 H. Kuhn and B. A. Wilson, Proc. Roy. Soc. (London) B63, 745 (1950).
- 14 Walter A MacNair, Phil. Mag. 2, 613 (1926).
- 15 The complete structure of  $\lambda 8446$  has been reported by D. O. Davis and K. W. Meissner in J. Opt. Soc. Am. 42, 871 (1952); the present measurements are in agreement with those of Davis and Meissner.
- 16 C. E. Moore, A Multiplet Table of Astrophysical Interest, Part I (Princeton: Princeton University Press, 1945).
- 17 J. C. Slater, Phys. Rev. 34, 1293 (1929).
- 18 E. U. Condon and G. H. Shortley, The Theory of Atomic Spectra (Cambridge, England: Cambridge University Press, 1935), p. 173.
- 19 H. Bethe, Handbuch der Physik, Vol. 24, No. 1, Chap. 3 (Berlin: Verlag Julius Springer, 1933), p. 432.

- 20 Bethe, op. cit., pp. 436-37. Bethe assumes that the effective potentials  $\bar{v}$  are the same for both states. The more general case for different potentials is easily inferred from Bethe's derivation.
- 21 Private communication.
- 22 Condon and Shortley, op. cit., p. 245.
- 23 Leo Goldberg, *Astrophys. J.* 82, 25 (1935).
- 24 Condon and Shortley, op. cit., Chap. 4.
- 25 C. E. Moore, Atomic Energy Levels, Vol. I (Washington, D.C.: National Bureau of Standards, 1949), p. 45.
- 26 John R. Holmes, *Phys. Rev.* 63, 41 (1943); Holmes, *J. Opt. Soc. Am.* 41, 360 (1951).
- 27 Bengt Edlen, *Kungl. Svenska Vetenskapsakademiens Handlingar*, Series 3, Vol. 20, No. 10 (1943).
- 28 Tolansky, op. cit., Chap. 15.
- 29 C. Runge and F. Paschen, *Ann. Phys. Chem.* 61, 647 (1897).
- 30 Condon and Shortley, op. cit., p. 245.